MINISTÉRIO DA CIÊNCIA E TECNOLOGIA
INSTITUTO NACIONAL DE PESQUISAS ESPACIAIS

INPE-15393-NTC/376

INCORPORATION OF THE UK MET OFFICE'S RADIATION SCHEME INTO CPTEC'S GLOBAL MODEL

Júlio Cesar Santos Chagas
Henrique de Melo Jorge Barbosa

Technical Note describing UK Met Office's radiative transfer code and its inclusion into CPTEC's atmospheric general circulation model

INPE
São José dos Campos
2008

PUBLICADO POR:

Instituto Nacional de Pesquisas Espaciais - INPE
Gabinete do Diretor (GB)
Serviço de Informação e Documentação (SID)
Caixa Postal 515 - CEP 12.245-970
São José dos Campos - SP - Brasil
Tel.:(012) 3945-6911/6923
Fax: (012) 3945-6919
E-mail: pubtc@sid.inpe.br

MINISTÉRIO DA CIÊNCIA E TECNOLOGIA
INSTITUTO NACIONAL DE PESQUISAS ESPACIAIS

INPE-15393-NTC/376

INCORPORATION OF THE UK MET OFFICE'S RADIATION SCHEME INTO CPTEC'S GLOBAL MODEL

Júlio Cesar Santos Chagas
Henrique de Melo Jorge Barbosa

Technical Note describing UK Met Office's radiative transfer code and its inclusion into CPTEC's atmospheric general circulation model

INPE
São José dos Campos
2008

ABSTRACT

The radiative transfer scheme of the UK Met Office (UKMO) Unified Model, developed by Edwards e Slingo (1996), was incorporated into the CPTEC's atmospheric general circulation model (AGCM), initially replacing the current operational short-wave scheme, based on Lacis e Hansen (1974) with water vapor absorption as in Ramaswamy e Freidenreich (1992), and afterwards replacing the operational long-wave scheme developed by Harshvardhan et al. (1987). This Technical Note describes the main characteristics of the UKMO scheme, the off-line tests performed against reference results for both shorwave and long-wave, the incorporation of the new scheme into CPTEC's AGCM and its impact on some aspects of the AGCM's climatology.

INCORPORAÇÃO DO ESQUEMA DE RADIAÇÃO DO UK MET OFFICE NO MODELO GLOBAL DO CPTEC

RESUMO

O esquema de transferência radiativa do modelo unificado do UK Met Office (UKMO), desenvolvido por Edwards e Slingo (1996), foi implantado no modelo de circulação geral atmosférica (MCGA) do CPTEC, substituindo inicialmente o esquema de ondas curtas atualmente em operação, baseado em Lacis e Hansen (1974) com a absorção pelo vapor de água segundo Ramaswamy e Freidenreich (1992), e depois substituindo o esquema operacional de ondas longas desenvolvido por Harshvardhan et al. (1987). Esta nota técnica descreve as principais características do esquema do UKMO, os testes *off-line* realizados para ondas curtas e para ondas longas, em comparação com resultados de referência, a incorporação do novo esquema no MCGA do CPTEC e o impacto dessa incorporação em alguns aspectos da climatologia do MCGA.

CONTENTS

Pág.

LIST OF FIGURES

LIST OF TABLES

1 INTRODUCTION **19**

2 UK MET OFFICE'S RADIATION CODE **23**

2.1 Spectral integration 23

2.2 Calculation of monochromatic fluxes 24

2.3 The calculation of fluxes 26

2.4 Rescaling of the single scattering properties 28

2.5 The calculation of the single scattering properties 28

2.6 Single scattering properties for individual processes 29

2.6.1 Gaseous absorption 29

2.6.2 Continuum absorption 30

2.6.3 Absorption and scattering by aerosols 30

2.6.4 Rayleigh scattering 30

2.6.5 Absorption and scattering by water droplets 31

2.6.6 Absorption and scattering by ice crystals 31

2.7 The treatment of overlapping gaseous absorption 31

2.8 The treatment of clouds 32

2.9 Remarks on algorithm 33

3 OFF-LINE COMPARISONS OF SHORT-WAVE CODES **37**

3.1 Gaseous extinction 37

3.1.1 Broad band comparisons 38

3.1.2 Summary of clear sky cases 38

3.2 Extinction by clouds 41

3.2.1 High cloud 42

3.2.2 Low cloud 42

3.2.3 Summary of cases with clouds 43

3.3 Extinction by aerosols 45

3.4 Concluding remarks 46

4 OFF-LINE COMPARISONS OF LONG-WAVE CODES 47
4.1 Cooling rate profiles 47
4.2 Long wave fluxes 47

5 INCORPORATION INTO CPTEC'S AGCM 53
5.1 Overview 53
5.2 Clouds 54
5.2.1 Condensate mixing ratio 54
5.2.2 Effective radius 55
5.2.3 Cloud cover and ice fraction 55
5.3 Aerosols 57

6 LONG-TIME RUNS WITH UKMO SHORT-WAVE CODE 61
6.1 Global means 61
6.2 Annual means 62

7 LONG-TIME RUNS WITH UKMO CODE 69
7.1 Short-wave fluxes 69
7.2 Long-wave fluxes 73
7.3 Processing time 76

8 CONCLUSION 79

REFERENCES 81

LIST OF FIGURES

Pág.

4.1 Long-wave cooling-rate profiles calculated by current operational code of CPTEC's AGCM, by UKMO-LW code, and by line-by-line code (FOMIN; GERSHANOV, 1996), for cases 25 to 34 of Ellingson et al. (1991) as described in Table 4.1. LBLRTM profiles for some cases are also plotted. First column, from top to bottom, displays results of cases 25, 27, 29, 31, and 33; second column, from top to bottom, displays results of cases 26, 28, 30, 32, and 34. 48
4.2 Same as Figure 4.1, except that pressure axis is logaritmic instead of linear. . 49
4.3 Net long wave fluxes at the surface calculated by current operational code of CPTEC's AGCM and by UKMO-LW code for cases 25 to 34 of Ellingson et al. (1991) as described in Table 4.1 . Pluses (+) and dashed lines represent the average and one standard deviation limits of results from an average of 36 different codes; stars represent the line-by-line results of Fomin e Gershanov (1996); red circles represent LBLRTM results. 50
4.4 Upward long wave fluxes at the top of atmosphere calculated by current operational code of CPTEC's AGCM and by UKMO-LW code for cases 25 to 34 of Ellingson et al. (1991) as described in Table 4.1 . Pluses (+) and dashed lines represent the average and one standard deviation limits of results from an average of 36 different codes; stars represent the line-by-line results of Fomin e Gershanov (1996); red circles represent LBLRTM results. 51

5.1 Effective radius for droplets (left) and ice crystals (right) according to the parametrization of Kiehl (1994). 56
5.2 Fraction of cloud condensed water which is as ice crystals as a function of layer temperature. 57

6.1 Annual mean of the clear-sky incident short wave at the surface (Wm^{-2}). Top: generated by NASA/GEWEX SRB Project; middle: calculated by current CPTEC AGCM and difference from SRB; bottom: calculated by CPTEC AGCM with UKMO short-wave code and difference from SRB. 63
6.2 Annual mean of the all-sky incident short wave at the surface (Wm^{-2}). Top: generated by NASA/GEWEX SRB Project; middle: calculated by current CPTEC AGCM and difference from SRB; bottom: calculated by CPTEC AGCM with UKMO short-wave code and difference from SRB. 64

6.3 Annual mean of the short-wave budget at the surface (Wm^{-2}). Top: generated by NASA/GEWEX SRB Project; middle: calculated by current CPTEC AGCM and difference from SRB; bottom: calculated by CPTEC AGCM with UKMO short-wave code and difference from SRB. 65
6.4 Annual mean of cloud cover (in percent). Top: generated by NASA/GEWEX SRB Project; middle: calculated by current CPTEC AGCM and difference from SRB; bottom: calculated by CPTEC AGCM with UKMO short-wave code and difference from SRB. 66
6.5 Annual mean of the total precipitation (mm day^{-1}). Top: measured by GPCP Project; middle: calculated by current CPTEC AGCM and difference from GPCP; bottom: calculated by CPTEC AGCM with UKMO short-wave code and difference from GPCP. 67

7.1 Annual mean of the all-sky incident short wave at surface (Wm^{-2}). Top: generated by NASA/GEWEX SRB project; middle: calculated by current CPTEC AGCM and difference from SRB, calculated by CPTEC AGCM with CLIRAD-SW short-wave code and difference from SRB; bottom: calculated by CPTEC AGCM with UKMO radiation code and difference from SRB. 70
7.2 Annual mean of the all-sky incident short wave at surface (Wm^{-2}). Top: generated by NASA/GEWEX SRB project; middle: calculated by current CPTEC AGCM and difference from SRB, calculated by CPTEC AGCM with CLIRAD-SW short-wave code and difference from SRB; bottom: calculated by CPTEC AGCM with UKMO radiation code and difference from SRB. 71
7.3 Annual mean of the all-sky net short wave at the surface (Wm^{-2}). Top: generated by NASA/GEWEX SRB project; middle: calculated by current CPTEC AGCM and difference from SRB, calculated by CPTEC AGCM with CLIRAD-SW short-wave code and difference from SRB; bottom: calculated by CPTEC AGCM with UKMO radiation code and difference from SRB. 72
7.4 Annual mean of the all-sky outgoing long wave at the top-of-atmosphere (Wm^{-2}). Top: generated by NASA/GEWEX SRB project, release 2.5; middle: calculated by current CPTEC AGCM and difference from SRB, calculated by CPTEC AGCM with CLIRAD-SW short-wave code and difference from SRB; bottom: calculated by CPTEC AGCM with UKMO radiation code and difference from SRB. 74
7.5 Annual mean of the all-sky net long wave at the surface (Wm^{-2}). Top: generated by NASA/GEWEX SRB project, release 2.5; middle: calculated by current CPTEC AGCM and difference from SRB, calculated by CPTEC AGCM with CLIRAD-SW short-wave code and difference from SRB; bottom: calculated by CPTEC AGCM with UKMO radiation code and difference from SRB. 75

7.6 Computational cost of CPTEC AGCM with Harshvardhan et al. (1987) and UKMO long-wave schemes, measured as the amount of floating pointing operations needed for a one day integration as a function of horizontal resolution (top) and number of vertical levels (bottom). 77
7.7 Comparison between optimized and original UKMO radiation scheme. Plot shows the user time necessary for a one day integration of CPTEC GCM with T62 horizontal resolution and time-steps of 600s, as a function of vertical resolution. 78

LIST OF TABLES

Pág.

3.1 Cases used for comparisons under clear (no clouds) and clean (no aerosols) conditions. TRO: tropical atmosphere, MLS: mid-latitude summer atmosphere. 38

3.2 **Case tro00.** Short wave radiation (in W/m^2) incident (InTA) and reflected (ReTA) at top-of-atmosphere, absorbed by atmosphere (AbAtm) and absorbed by surface (AbSfc), and corresponding partition fractions (α_p = ReTA/InTA, α_{atm} = AbAtm/InTA e α_{sfc} = AbSfc/InTA) for tropical atmosphere, solar zenith angle 0.0 degreee and surface albedo 0.2. 39

3.3 **Case tro60.** Short wave radiation (in W/m^2) incident (InTA) and reflected (ReTA) at top-of-atmosphere, absorbed by atmosphere (AbAtm) and absorbed by surface (AbSfc), and corresponding partition fractions (α_p = ReTA/InTA, α_{atm} = AbAtm/InTA e α_{sfc} = AbSfc/InTA) for tropical atmosphere, solar zenith angle 59.973 degreee and surface albedo 0.2. 39

3.4 **Case tro75.** Short wave radiation (in W/m^2) incident (InTA) and reflected (ReTA) at top-of-atmosphere, absorbed by atmosphere (AbAtm) and absorbed by surface (AbSfc), and corresponding partition fractions (α_p = ReTA/InTA, α_{atm} = AbAtm/InTA e α_{sfc} = AbSfc/InTA) for tropical atmosphere, solar zenith angle 75.4629 degreee and surface albedo 0.2. 39

3.5 **Case mls00.** Short wave radiation (in W/m^2) incident (InTA) and reflected (ReTA) at top-of-atmosphere, absorbed by atmosphere (AbAtm) and absorbed by surface (AbSfc), and corresponding partition fractions (α_p = ReTA/InTA, α_{atm} = AbAtm/InTA e α_{sfc} = AbSfc/InTA) for mid-latitude summer atmosphere, solar zenith angle 0.0 degreee and surface albedo 0.2. 40

3.6 Partition of incident short-wave radiation (among reflected at top-of-atmosphere, absorbed by atmosphere and absorbed by surface) for clear-sky cases. Line-by-line LBLRTM+CHARTS results are shown in the second column; figures for broad-band codes CPT-old, CPT-new, CLIRAD and UKMO are differences of their results from line-by-line; cases are as described in Table 3.1. 40

3.7 Cases used for comparisons under cloudy conditions. For all cases: tropical atmosphere, surface albedo 0.2 and overcast sky with clouds of liquid droplets of effective radius of 10 μm. 41

3.8 **Case high00.** Short wave radiation (in W/m^2) incident (InTA) and reflected (ReTA) at top-of-atmosphere, absorbed by atmosphere (AbAtm) and absorbed by surface (AbSfc), and corresponding partition fractions (α_p = ReTA/InTA, α_{atm} = AbAtm/InTA e α_{sfc} = AbSfc/InTA) for tropical atmosphere, solar zenith angle 0.0 degreee, surface albedo 0.2 and an overcast cloud between 10.5 and 11.0 km. 42
3.9 **Case high60.** Short wave radiation (in W/m^2) incident (InTA) and reflected (ReTA) at top-of-atmosphere, absorbed by atmosphere (AbAtm) and absorbed by surface (AbSfc), and corresponding partition fractions (α_p = ReTA/InTA, α_{atm} = AbAtm/InTA e α_{sfc} = AbSfc/InTA) for tropical atmosphere, solar zenith angle 59.973 degreee, surface albedo 0.2 and an overcast cloud between 10.5 and 11.0 km. 42
3.10 **Case high75.** Short wave radiation (in W/m^2) incident (InTA) and reflected (ReTA) at top-of-atmosphere, absorbed by atmosphere (AbAtm) and absorbed by surface (AbSfc), and corresponding partition fractions (α_p = ReTA/InTA, α_{atm} = AbAtm/InTA e α_{sfc} = AbSfc/InTA) for tropical atmosphere, solar zenith angle 75.4629 degreee, surface albedo 0.2 and an overcast cloud between 10.5 and 11.0 km. 43
3.11 **Case low00.** Short wave radiation (in W/m^2) incident (InTA) and reflected (ReTA) at top-of-atmosphere, absorbed by atmosphere (AbAtm) and absorbed by surface (AbSfc), and corresponding partition fractions (α_p = ReTA/InTA, α_{atm} = AbAtm/InTA e α_{sfc} = AbSfc/InTA) for tropical atmosphere, solar zenith angle 0.0 degreee, surface albedo 0.2 and an overcast cloud between 3.5 and 4.0 km. 43
3.12 **Case low60.** Short wave radiation (in W/m^2) incident (InTA) and reflected (ReTA) at top-of-atmosphere, absorbed by atmosphere (AbAtm) and absorbed by surface (AbSfc), and corresponding partition fractions (α_p = ReTA/InTA, α_{atm} = AbAtm/InTA e α_{sfc} = AbSfc/InTA) for tropical atmosphere, solar zenith angle 59.973 degreee, surface albedo 0.2 and an overcast cloud between 3.5 and 4.0 km. 44
3.13 **Case low75.** Short wave radiation (in W/m^2) incident (InTA) and reflected (ReTA) at top-of-atmosphere, absorbed by atmosphere (AbAtm) and absorbed by surface (AbSfc), and corresponding partition fractions (α_p = ReTA/InTA, α_{atm} = AbAtm/InTA e α_{sfc} = AbSfc/InTA) for tropical atmosphere, solar zenith angle 75.4629 degreee, surface albedo 0.2 and an overcast cloud between 3.5 and 4.0 km. 44

3.14 Partition of incident short-wave radiation (among reflected at top-of-atmosphere, absorbed by atmosphere and absorbed by surface) for cloudy-sky cases. Line-by-line LBLRTM+CHARTS results are shown in the second column; figures for broad-band codes CPT-old, CPT-new, CLIRAD and UKMO are differences of their results from line-by-line; cases are as described in Table 3.7. 45

4.1 Cases from Ellingson et al. (1991) used for comparison between different long-wave codes. 47

5.1 Composition of each atmospheric region as total column amounts (*aermass*) of each aerosol type given in kg/m^2. BL means boundary layer. 58

5.2 Composition of the two aerosol profiles given as mixing ratios $mixr(k, j)$ of each one of the five aerosol types from the climatology. Figures are in 10^{-10} and , in the stratosphere, $p_\star$ was made equal to $p_\circ$. 60

6.1 Global mean solar radiation budgets (in Wm^{-2}) for CPTEC AGCM. CPTEC-old: original model with Davies (1982) formulation; CPTEC-new: current operational model with Ramaswamy e Freidenreich (1992) formulation; UKMO: current model with Edwards e Slingo (1996) short-wave code; Wild05and Wild06: figures taken from Wild (2005) and Wild et al. (2006); SRB: NASA/GEWEX SRB dataset (WHITLOCK et al., 1993). 61

7.1 Global mean of short-wave fluxes (in Wm^{-2}) at top-of-atmosphere (TOA) and at surface (SFC) averaged over 1) a twelve-month (Dec/2002–Nov/2003) period, and two three-month periods, 2) Dec/2002–Feb/2003 and 3) Jun/2003–Aug/2003. SRB, CPTEC, CLIRAD and UKMO as described in the text. . . . 73

7.2 Global mean of long-wave fluxes (in Wm^{-2}) at top-of-atmosphere (TOA) and at surface (SFC) averaged over 1) a twelve-month (Dec/2002–Nov/2003) period, and two three-month periods, 2) Dec/2002–Feb/2003 and 3) Jun/2003–Aug/2003. SRB, CPTEC, CLIRAD and UKMO as described in the text. . . . 76

1 INTRODUCTION

Harshvardhan et al. (1987) developed a set of routines for the parameterization of radiative transfer in atmospheric general circulation models (AGCM). This scheme was incorporated into COLA's (Center for Ocean-Land-Atmosphere Studies, Maryland, United States) AGCM by Sato et al. (1989) and Hou (1990). They replaced the formulation of Lacis e Hansen (1974) for the absorption of solar radiation by water vapor, part of Harshvardhan et al.'s scheme, with the formulation of Davies (1982) which was supposed to obtain nearly the same short-wave fluxes with less computational cost. This radiation scheme was described by Chagas e Tarasova (1996) and became operational at CPTEC when COLA's AGCM was implemented there in the early nineties.

Plana-Fattori et al. (1997) used an off-line version of the short-wave scheme of CPTEC's AGCM to explore the effects of substituting the formulations of Davies with the original formulation of Lacis and Hansen and with the formulations of Briegleb (1992), Ramaswamy e Freidenreich (1992) and Chou e Lee (1996). They used the standard atmospheres of McClatchey et al. (1972) and compared their results with line-by-line results publisehd by Fouquart et al. (1991). Their main conclusions were that top-of-the-atmosphere and surface fluxes obtained with the formulations of Lacis & Hansen and Davies are very similar but both sistematically subestimate the amount of solar radiation absorbed by the atmosphere if compared to line-by-line results; moreover, Davies's formulation generates unrealistic oscillations on the heating rate profiles; also, the three remaining formulations significantly reduce but don't eliminate the subestimation of atmospheric short-wave absorption. Souza et al. (1997) compared mean fields obtained with two one-month integrations of CPTEC's AGCM using the same initial conditions, one with Davies's formulation and other with Chou and Lee's one. The configuration of several large scale fields came closer to observed fields when Chou and Lee's formulation replaces Davies's one.

Climate characteristics of CPTEC's global model were analized by Cavalcanti et al. (2002), who confirmed its deficiencies in simulating observed radiative fluxes and suggested that its radiation and cloud schemes should be improved. Tarasova e Cavalcanti (2002) showed that CPTEC's AGCM sistematically overestimate incident short-wave flux at surface if compared to satellite-derived estimates.

In 2004, Ramaswamy and Freidenreich's formulation became operational at CPTEC (CHAGAS et al., 2004), replacing Davies's one and lowering the excess of incident short wave at the surface. In parallel, efforts are being made in testing and implementing modern radiation schemes into CPTEC's global model. Apart from obtaining more realistic simulation of the partition of solar radiation within the earth-atmosphere system, other aims of that effort are to improve the parameterization of cloud-radiation interactions and to allow the inclusion of the effects of aerosols and trace gases. One of these efforts, the incorporation into CPTEC's AGCM of the short-wave scheme of Chou e Suarez (1999), known as CLIRAD, as modified by Tarasova e Fomin (2000), is described by Tarasova et al. (2007).

This Technical Note describes the incorporation of the operational radiation scheme of the UK Met Office's (Exeter, UK) Unified Model, developed by Edwards e Slingo (1996), for both short-wave and long-wave calculations, into CPTEC's AGCM.

Chapter 2 presents a description of the UKMO radiation code, focussing on the core code which is used for both short-wave and long-wave spectral bands. Details are shown on how the code works in an atmospheric column, how the individual extinction processes are treated and how their effects are combined to obtain fluxes and heating rates.

Prior to the incorporation into an AGCM, radiative transfer schemes should be tested in off-line mode by comparing their output with reference results usually obtained with line-by-line calculations. Chapters 3 and 4 present and discuss the off-line comparisons carried out with the short-wave and long-wave applications of UKMO code, respectively.

When estimating the radiative effects of clouds, current CPTEC's AGCM radiative code use as input the cloud cover fraction and combine it with other model variables to estimate cloud optical thickness. Differently, UKMO code also requires as input the effective radius of cloud particles, the mixing ratio of condensed water and the ratio (ice fraction) between ice and liquid water amounts within the cloud. When incorporating the new code, it was then necessary to incorporate a cloud microphysics scheme to generate these other parameteres. There was also the intention of taking into account the effect of aerosols on radiative transfer parametrization and a simplified aerosol climatology was implemented Cusack et al. (1998). Chapter 5 describes technicalities about the incorporation of the UKMO code into CPTEC's AGCM and the main characteristics of the cloud microphysics scheme and of the aerosol climatology.

Once tested in off-line mode, the UKMO radiative code was incorporated into CPTEC's AGCM in two steps. Initially, this was done only for short-wave calculations. In Chapter 6 some mean fields obtained from long-term runs of the AGCM with the new short-wave code were compared to those obtained with the current operational AGCM. The second step was the incorporation of the UKMO scheme for long-wave calculations. Chapter 7 compares mean fields obtained from long-term runs of the AGCM with UKMO code for both short-wave and long-wave calculations, with current radiation code for both bands, and with CLIRAD for short wave. General conclusions are drawn and presented in Chapter 8.

2 UK MET OFFICE'S RADIATION CODE

The radiation code inside an AGCM is a set of routines which act upon a set of atmospheric columns. It reads atmospheric profiles of model variables (temperature, pressure and humidity) and atmospheric constituents (gases, clouds, aerosols) and evaluates radiative fluxes and the resulting heating rates. In some models (e.g. current CPTEC/INPE and ECMWF operational models), short-wave and long-wave codes are completely distinct. This does not happen with UKMO radiation code which has a common core used for both spectral regions. Other interesting characteristic of this code are the so called "spectral files", one for short wave and other for long wave. These files define the limits of the spectral bands inside each spectral region, which gases and aerosols are active in each band and the necessary parameters to evaluate the optical properties of each atmospheric layer. Such arrangement allows updates in the parameterizations with no need for updating or recompiling the routines. More detail on spectral files can be found in an unpublished document provided by John Edwards of the UK Met Office (EDWARDS; THELEN, 2003). The following description of the code follows closely another unpublished document also provided by John Edwards (EDWARDS et al., 2003). It refers mainly to the core code used for both short-wave and long-wave spectral regions.

UKMO radiation code allows the calculation of fluxes —using two-stream techniques— or radiances —using spherical harmonics. For AGCM applications, only fluxes are required and the overall sequence of procedures for two-stream calculations is described here. Initially, spectrally independent calculations related to moist aerosols and cloud overlap are performed. Then the fluxes are calculated in each spectral band to increment the broad-band fluxes. Within each band, the first to be calculated are the single scattering properties, uniform across the band, of radiatively active species other than gases, and gaseous scaling functions independent of the k-term. Depending on the option chosen for treating overlapping gaseous absorption, a different routine is called to generate a set of pseudo-monochromatic calculations. In each of these calculations, the final single scattering properties, including contributions from gases, are assembled and again a separate routine is called depending on the treatment of cloud overlap. Then the linear two-stream equations are assembled and solved.

2.1 Spectral integration

The radiative fluxes are determined as a sum of quasi-monochromatic calculations using a two-stream approximation (upward and downward diffuse fluxes plus direct solar flux). The symbol F is used for flux (direct, diffuse or net). Inside each spectral band, only the mass coefficient of gaseous absorption is made frequency-dependent. The total flux is given by:

$$F = \sum_j F_j^{(b)}, \tag{2.1}$$

where j refers to each extinction process and the flux $F_j^{(b)}$ in each spectral band (b) is

$$F_j^{(b)} = \sum_k w_k F_k^{(qm)}. \tag{2.2}$$

Index k refers to quasi-monochromatic regions (qm) inside the band and w_k is the weight attributed to each region. The number of quasi-monochromatic calculations and the weigths w_k are determined by the method adopted for treating overlapping gaseous absorption and by the data in the spectral file.

2.2 Calculation of monochromatic fluxes

The atmospheric column is divided into N homogeneous layers, numbered from 1 to N, starting from the top. Their limits are $N+1$ levels numbered from 0 to N, according to the schematic below.

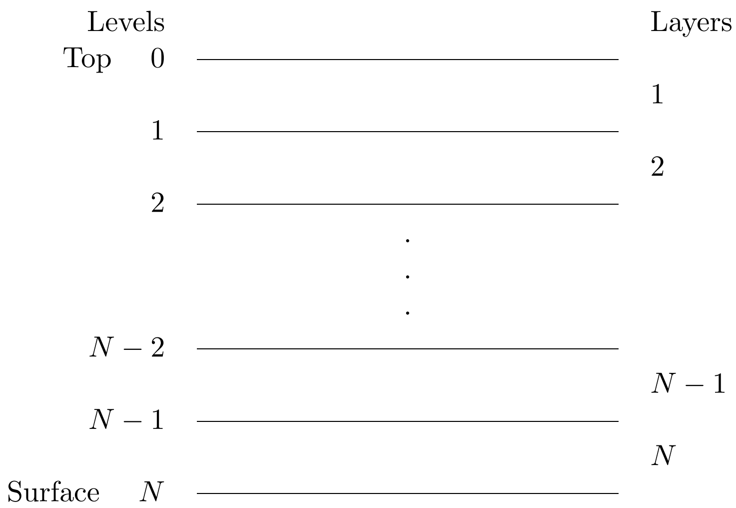

The basic variables in the solar region are the upward flux U, the total downward (diffuse plus direct) flux V, and the direct solar flux Z. In the infra-red, U is the upward flux minus πB (B is the Plankian function) and V is the downward flux minus πB. When only heating rates are required, the net flux, $N = V - U$, is used.

The fluxes in a column of homogeneous layers are given by:

$$
\begin{aligned}
U_{i-1} &= T_i U_i + R_i V_{i-1} + S_i^+ \\
V_i &= T_i V_{i-1} + R_i U_i + S_i^- \\
Z_i &= T_{0i} Z_{i-1}
\end{aligned}
\tag{2.3}
$$

T and R are the diffuse transmission and reflection coefficients, T_0 is the direct transmission coefficient, and S^+ and S^- are source terms. The subscripts on fluxes refer to levels and those on T, R , T_0 and S refer to layers:

$$
\begin{array}{lcr}
 & \uparrow U_{i-1} & \\
\text{level } i\text{-1} & \overline{\hspace{8cm}} & \\
 & \downarrow V_{i-1} \quad \downarrow Z_{i-1} & \\
 & T_i\ ,\ R_i\ ,\ T_{0i}\ ,\ S_i^+\ ,\ S_i^- & \text{layer } i \\
 & \uparrow U_i & \\
\text{level } i & \overline{\hspace{8cm}} & \\
 & \downarrow V_i \quad \downarrow Z_i &
\end{array}
$$

At the top of the atmosphere, the boundary condition for solar radiation is $V_0 = Z_0 = \Phi_0/\chi_0$, where Φ_0 is the solar irradiance in the band and χ_0 is the secant of the solar zenith angle; in the infra-red, the boundary condition is $V_0 = 0$. At the surface the appropriate boundary condition on the shortwave fluxes is

$$
\begin{aligned}
U_N &= (\alpha_s - \alpha_d) Z_N + \alpha_d V_N \\
&= \alpha_s Z_N + \alpha_d (V_N - Z_N)
\end{aligned}
\tag{2.4}
$$

where α_s and α_d are the surface albedos for direct and diffuse radiation. In the infra-red

$$U_N = \alpha_d V_N + \epsilon_* \pi B_* \tag{2.5}$$

where ϵ_* is the emissivity of the surface and B_* is the corresponding Planckian function.

Source terms are due to the scattering of direct solar beam into diffuse radiation and to variations in the Planckian source function across the layer:

$$S_i^+ = c_{1i} Z_{i-1} \quad \text{and} \quad S_i^- = c_{2i} Z_{i-1} \tag{2.6}$$

for short wave and

$$S_i^+ = c_{1i}\Delta_{1i} + c_{2i}\Delta_{2i} \text{ and } S_i^- = -c_{1i}\Delta_{1i} + c_{2i}\Delta_{2i} \tag{2.7}$$

for long wave. The c_j depend on layer properties and

$$\begin{aligned} \Delta_{1i} &= B_i - B_{i-1} \\ \Delta_{2i} &= 2(B_i + B_{i-1} - 2B_i^{(m)}) \end{aligned} \tag{2.8}$$

where B is the Planckian function integrated across the band at the appropriate level and $B_i^{(m)}$ is the Planckian function at the middle of the i^{th} layer. B is given by a polynomial:

$$B = \sum_{k=0}^{n} \beta_k (\theta/\theta_R)^k. \tag{2.9}$$

2.3 The calculation of fluxes

The fundamental single scattering properties of a layer are the optical depth τ, the albedo of single scattering ω, and the asymmetry g. T, T_0, R and c_j depend on the optical properties of the layer and are obtained by a two-stream approximation expressed in terms of the diffuse fluxes, $F^{\pm}$:

$$\frac{dF^+}{d\tau} = \alpha_1 F^+ - \alpha_2 F^- - Q^+ \tag{2.10}$$

$$\frac{dF^-}{d\tau} = \alpha_2 F^+ - \alpha_1 F^- - Q^- \tag{2.11}$$

where $Q^{\pm}$ are source terms. Values of $s = \alpha_1 + \alpha_2$ and $d = \alpha_1 - \alpha_2$ are obtained in different ways depending on the chosen two-stream approximation. The code allows for different approximations.

In Eddington's approximation,

$$\begin{aligned} s &= D - \frac{3}{2}\omega g \\ d &= D(1-\omega) \end{aligned} \tag{2.12}$$

In the approximation by Zdunkowski e Korb (1985),

$$\begin{aligned} s &= 2 - \frac{3}{2}\omega g - \frac{1}{2}\omega \\ d &= 2(1-\omega) \end{aligned} \tag{2.13}$$

where D is the diffusivity factor, taken as 2. In the original version of Zdunkowski et al. (1980),

$$\begin{aligned} s &= 2 - \frac{3}{2}\omega g - \frac{1}{2}\omega \\ d &= 2(1-\omega) \end{aligned} \tag{2.14}$$

Using discrete ordinates,

$$\begin{aligned} s &= \sqrt{3}(1-\omega g) \\ d &= \sqrt{3}(1-\omega) \end{aligned} \tag{2.15}$$

Using the hemispheric mean approximation,

$$\begin{aligned} s &= 2(1-\omega g) \\ d &= 2(1-\omega) \end{aligned} \tag{2.16}$$

The diffuse transmission and reflection coefficients are then calculated:

$$\begin{aligned} \lambda &= \sqrt{sd} \\ p &= e^{-\lambda\tau} \\ \Gamma &= \frac{s-\lambda}{s+\lambda} \\ T &= \frac{p(1-\Gamma^2)}{1-p^2\Gamma^2}) \\ R &= \frac{\Gamma(1-p^2)}{1-p^2\Gamma^2} = \Gamma(1-pT) \end{aligned} \tag{2.17}$$

The c_j are calculated diferently for short and for long waves. For long waves,

$$\begin{aligned} c_1 &= \frac{1-T+R}{s\tau} \\ c_2 &= -\frac{1}{s\tau}\left[1+R+T-2\frac{1-T-R}{\tau d}\right] \end{aligned} \tag{2.18}$$

The indeterminacy which occurs in the limit $\tau \to 0$ is removed by adding a small tolerance to the terms $s\tau$, $d\tau$, $1-T+R$, and $1+R+T$. To define the c_j in the solar region it is defined the quantity

$$\xi_0 = \frac{3g}{2\chi_0} \tag{2.19}$$

for the two-stream approximations above, except for the discrete ordinate approximation, when

$$\xi_0 = \frac{\sqrt{3}g}{\chi_0} \tag{2.20}$$

Afterwards it is defined

$$f = \omega\frac{\chi_0}{2} \tag{2.21}$$

$$\begin{aligned} \nu_+ &= f(S - \chi_0 - \xi_0(d - \chi_0)) \\ \nu_- &= f(S + \chi_0 + \xi_0(d + \chi_0)) \end{aligned} \tag{2.22}$$

And, at last,

$$\begin{aligned} c_1 &= (\nu_+ - R(1 + \nu_-)) - \nu_+ T T_0 \\ c_2 &= T_0(1 + \nu_- - R\nu_+) - (1 + \nu_-)T \end{aligned} \tag{2.23}$$

2.4 Rescaling of the single scattering properties

The innacuracies in the representation of scattering, due to the use of two-stream approximations, can be substantially reduced by the δ-rescaling transformation of Joseph et al. (1976) used in the code. A forward scattering fraction f is defined, using the standard prescription $f = g^2$, and the single scattering properties are rescaled using the transformation

$$\begin{aligned} \tau &\rightarrow \tau(1 - \omega f) \\ \omega &\rightarrow \omega(1 - f)/(1 - \omega f) \\ g &\rightarrow (g - f)/(1 - f) \end{aligned} \tag{2.24}$$

2.5 The calculation of the single scattering properties

The single scattering properties related to the physical sources are the mass extinction and scattering coefficients, $k^{(e)}$ and $k^{(s)}$, and the asymmetry g. When different optical processes are active in a region the contributions from each of them are combined by:

$$\begin{aligned}
k^{(e)} &= \sum_j k_j^{(e)}, \\
k^{(s)} &= \sum_j k_j^{(s)}, \\
g &= \sum_j k_j^{(s)} g_j / \sum_j k_j^{(s)} \\
f &= \sum_j k_j^{(s)} f_j / \sum_j k_j^{(s)}
\end{aligned} \tag{2.25}$$

where, for each process, indexed by j, $f_j = g_j^2$. The optical depth and single scattering albedo are then determined:

$$\begin{aligned}
\tau &= k^{(e)} \Delta m \\
\omega &= \frac{k^{(s)}}{k^{(e)} + k^{(s)}}
\end{aligned} \tag{2.26}$$

where Δm is the column mass in the layer.

2.6 Single scattering properties for individual processes

2.6.1 Gaseous absorption

In a spectral band with M absorbing gases, each one is taken into account in a quasi-monochromatic calculation with an effective mass extinction coefficient $K_j^{(g)}$, calculated at reference temperature and pressure. The total contribution to the mass extinction coefficient is

$$k^{(e,g)} = \sum_j^M K_j^{(g)} q_j f_j(p, \theta) \tag{2.27}$$

where q_j is the mixing ratio of the j^{th} gas and f_j is the scaling function, which allows for variations in the pressure and the temperature. Two forms for f are allowed:

$$f = \left(\frac{p + \Delta}{p_0 + \Delta}\right)^{\alpha} \left(\frac{\theta}{\theta_0}\right)^{\beta} \text{and} \tag{2.28}$$

$$f = \left(\frac{p + \Delta}{p_0 + \Delta}\right)^{\alpha} \left[1 + A\left(\frac{\theta - \theta_0}{\theta_0}\right) + B\left(\frac{\theta - \theta_0}{\theta_0}\right)^2\right]. \tag{2.29}$$

The parameters α,β, Δ, A and B are determined by fitting to gaseous transmission data and are chosen such that $f = 1$ if they are given values of 0. p_0 and θ_0 are the reference pressure and temperature. Δ represents the effects of Doppler broadening. The scaling function and the parameters are read from the spectral file.

2.6.2 Continuum absorption

The self- and foreign-broadened continua of water vapor are included. Their contribution to the mass extinction coefficient is

$$k^{(e,c)} = K_f^{(c)} q_w f_f n_{bf} + K_s^{(c)} q_w f_s n_{bs} \tag{2.30}$$

where q_w is the mixing ratio of water vapour, f is the scaling function and n_b is the molar density of the appropriate broadening species (water vapor for self- and other species for foreign-broadened continua). The subscripts f and s stand for the foreign and self-broadened continua respectively. The coefficients $K_f^{(c)}$ and $K_s^{(c)}$ are determined externally by fitting and read from the spectral file. The model used for the continuum is based on the CKD model of Clough et al. (1989) and the necessary parameters are updated by modifying the spectral file.

2.6.3 Absorption and scattering by aerosols

The contributions of each species of aerosol in each spectral band to the total and scattering extinctions are set proportional to the mass mixing ratio of the aerosol: the constants of proportionality and the asymmetry are determined externally and read from the spectral file. There is no allowance for variations in the shape of the size distribution.

$$\begin{aligned} k^{(e,a)} &= \sum_j K_j^{(e,a)} q_j, \\ k^{(s,a)} &= \sum_j K_j^{(s,a)} q_j, \\ g^{(a)} &= \sum_j K_j^{(s,a)} q_j g_j / k^{(s,a)} \end{aligned} \tag{2.31}$$

where the sum is taken over all the species of aerosols and q_j are the mixing ratios. Parametrizations of the influence of humidity on the optical properties of hygroscopic aerosols are included by the use of a look-up table in the humidity which is read from the spectral file.

2.6.4 Rayleigh scattering

Rayleigh scattering is represented by adding to the scattering and total extinctions a constant value for each spectral band, determined externally and read from the spectral file.

2.6.5 Absorption and scattering by water droplets

The single scattering properties in a water cloud depend on the mass mixing ratio of liquid water L and on the effective radius of the droplets r_{el}. The parameterization of Slingo e Schrecker (1982) is used:

$$\begin{aligned} k^{(e)} &= L(a + b/r_{el}) \\ k^{(s)} &= k^{(e)}(1 - c - dr_{el}) \\ g &= e + fr_{el} \end{aligned} \tag{2.32}$$

where the constants $a, \ldots, f$, which vary with spectral band, are determined externally and read from the spectral file.

2.6.6 Absorption and scattering by ice crystals

The treatment of scattering by ice crystals is similar to that used for water vapour and has the same form of the parameterization of Slingo e Schrecker (1982):

$$\begin{aligned} k^{(e)} &= I(a + b/r_{ei}) \\ k^{(s)} &= k^{(e)}(1 - c - dr_{ei}) \\ g &= e + fr_{ei} \end{aligned} \tag{2.33}$$

where r_{ei} is the effective radius of the crystals and the constants $a, \ldots, f$ are determined externally and read from the spectral file.

2.7 The treatment of overlapping gaseous absorption

An efficient method, proposed by Ritter e Geleyn (1992) and extended by Edwards (1996), known as equivalent extinction, is used for treating the overlapping gaseous absorption. The effects of minor gases are represented by a single absorption coefficient within the band, which is determined for the local atmospheric conditions by a subsidiary calculation.

In the infra-red region, supposing a minor gas to have k-terms K_r, $r = 1, \ldots, n$, the net flux N_r is calculated including just absorption by the r^{th} k-term of the gas (and any non-cloudy grey absorption). The equivalent extinction is defined as

$$\bar{K} = \sum_r w_r K_r N_r / \sum_r w_r N_r \tag{2.34}$$

where the w_r are the corresponding weights. As fluxes are calculated on levels, the equivalent extinction is calculated using the mean net flux in the layer, wich is taken as a simple average of the values at the boundaries.

In the solar region, direct and diffuse radiation are treated separately. Direct transmissions for each minor gas can be calculated and are multiplicative, and the direct flux can be calculated precisely. For the diffuse fluxes, the absorption by the minor gas is considered to occur into regions of strong absorption, where the radiation scattered into the diffuse beam effectively vanishes, and of weak absorption, where it can be treated as grey. The equivalent extinction for diffuse radiation is taken as uniform

$$\bar{K} = \sum_r w_r K_r Z_{*r} / \sum_r w_r Z_{*r} \tag{2.35}$$

where Z_{*r} is the direct flux at the surface for the r^{th} k-term.

2.8 The treatment of clouds

Within any atmospheric layer, i, a fractional cloud cover, W_i, may be specified. This cloud is divided into N_T *types*, each constituting a fraction, ϕ_j , of the total amount of cloud. Each of these sub-clouds is made up of mixtures of various *components*. The rule which determines how the components are partitioned between the types of cloud is called a *representation*. Clouds consist of four components: stratiform water, stratiform ice, convective water and convective ice. Mixed-phase clouds may be represented as homogeneous, in which case there are two types, stratiform and convective, with homogeneous mixtures of water and ice in each; or as segregated, in which case there are four types of clouds, each consisting of a different component.

Clouds are treated as plane-parallel. The overlapping of clouds in the vertical uses a generalization of the algorithm described by Geleyn e Hollingsworth (1979) and Zdunkowski et al. (1982). In a layer, individual types of cloud are aggregated into regions. Within each region the fluxes are horizontally uniform and, at the boundary between layers, are tranferred from one region to another in accordance with the assumption on overlaps. There are two ways of decomposing the layer into regions. All clouds may be aggregated into one region, thus splitting the layer into clear and cloudy parts, or the convective and stratiform clouds may be aggregated into separate regions, thus giving three regions and maintaining the vertical coherence of convective cloud.

The overlapping is represented by the coefficients used to couple fluxes at the boundaries of layers. For the upward flux:

$$\hat{U}_{ij} = \sum_k u_{ijk} \check{U}_{ik} \tag{2.36}$$

where U_{ij} denotes the upward flux in the j^{th} region at the i^{th} level, with the circumflex denoting a value just above the boundary and the háček a value just below it. For the downward flux:

$$\hat{V}_{ij} = \sum_k v_{ijk} \check{V}_{ik} \tag{2.37}$$

with an identical equation for Z. If X_{ij} denotes the area within the i^{th} layer covered by the j^{th} region and Y_{ijk} the area on the i^{th} level where the j^{th} region overlies the k^{th}, generally,

$$u_{ijk} = Y_{ikj}/X_{i+1,j} \tag{2.38}$$

and

$$v_{ijk} = Y_{ikj}/X_{i,j} \tag{2.39}$$

The Y_{ijk} are determined by the assumption on the overlap. For *random overlap*:

$$Y_{ijk} = X_{ij}X_{i+1,j} \tag{2.40}$$

For *maximum-random overlap*, similar regions are maximally overlapped, but dissimilar ones are randomly overlapped:

$$Y_{ijk} = \min(X_{ij}, X_{i+1,j}) \tag{2.41}$$

and, if $k \neq j$,

$$Y_{ijk} = (X_{ij} - Y_{ijj})(X_{i+1,k} - Y_{i+1,kk}) \tag{2.42}$$

Where $X_{ij} = 0$, u_{ijk} is undefined, and its value does not affect the radiative fluxes, but it is necessary to assign a value for the execution of the subsequent algorithm. In such cases u_{ijk} and v_{ijk} are set to 1 if $j = k$ and 0 otherwise.

2.9 Remarks on algorithm

The two-stream equations are a set of linear simultaneous equations which generates a band matrix containing a significant proportion of zeros even along those diagonals with non-zero elements. The most efficient and accurate method to solve these equations is to create a set of algebraic recurrences, like a Gaussian elimination, in order to reduce the number of required operations. Initially, a set of relations between the upward flux just above the boundary of a layer and the downward fluxes just below it is generated:

$$\hat{U}_{ij} = \sum_k \alpha_{i+1,jk} \check{V}_{ik} + G^{+}_{i+1,j} \tag{2.43}$$

where the notation is the same used in the previous section on clouds, α is a generalized albedo and G^+ is independent of U and V. At the surface, G^+ includes the solar term. Then, using U for $\hat{U}$ and V for $\check{V}$, V (from equation 2.3) is substituted into the preceding equation:

$$U_{ij} = \sum_k \alpha_{i+1,jk} \big[\sum_l v_{ikl} (T_{il} V_{i-1,l} + R_{il} U_{il} + S^-_{ik}) \big] + G^+_{i+1,j} \tag{2.44}$$

It is defined

$$\theta_{ijl} = \sum_k \alpha_{i+1,jk} v_{ikl} \tag{2.45}$$

so that

$$\sum_l (\delta_{jl} - \theta_{ijl} R_{il}) U_{il} = \sum_l \theta_{ijl} T_{il} V_{i-1,k} + \sum_l \theta_{ijl} S^-_{il} G^+_{i+1,j} \tag{2.46}$$

which is of the form

$$\sum_l \beta_{ijl} U_{il} = \sum_l \gamma_{ijl} V_{i-1,l} + H^+_{ij} \tag{2.47}$$

and by taking linear combinations of these equations as necessary it can be ensured that $\beta_{ijl} = 0$ whenever $l > j$. The equation for the upward fluxes

$$U_{i-1,j} = \sum_k u_{i-1,jk} (T_{ik} U_{ik} + R_{ik} V_{i-1,k} + S^+_{ik}) \tag{2.48}$$

is of the form

$$U_{i-1,j} = \sum_k \zeta_{ijk} U_{ik} + \sum_k \alpha_{ijk} V_{i-1,k} + G^+_{ij} \tag{2.49}$$

Using that equation U may be eliminated from the right to obtain an equation of the original form with i replaced by $i-1$. It is then possible to perform back substitution. If the downward fluxes just above the i-th boundary level, $\hat{V}_{ij}$, are known, it is possible to calculate the downward fluxes just below the boundary using the coefficients v_{ijk}. The upward fluxes just below the boundary may be determined from

$$\sum_l \beta_{ijl} U_{il} = \sum_k \gamma_{ijl} V_{i-1,l} + H^+_{ij} \tag{2.50}$$

The downward fluxes at the base of the layer may now be determined from the equations of transfer, completing the recurrence.

In the long wave, scattering is not so important as in the short wave and its effects may be treated approximately. The transmission and reflection coefficients of the layers are calculated including the effects of scattering, but the equations of transfer are solved using the first two stages of an iterative scheme. Assuming that the upward flux at a level in the atmosphere is Planckian at the local temperature, it is possible to calculate the downward differential flux setting the upward differential flux to zero and transmitting them down from the top of the atmosphere. Knowing the downward differential fluxes at each level, it is possible to work upwards through the atmosphere calculating the upward fluxes.

3 OFF-LINE COMPARISONS OF SHORT-WAVE CODES

This chapter is a summary of an unpublished document, written in portuguese, which was handed out to the members of the Modeling Committee of CPTEC in December 2006 (CHAGAS, 2006).

Radiation codes used in general circulation models are usually validated by comparing their results with reference results obtained from line-by-line models, which explicitly take into account the laboratory-obtained characteristics of hundreds of thousands absorption lines of atmospheric gases. In recent decades there have been international intercomparison programs — e.g. the ICRCCM, InterComparison of Radiation Codes used in Climate Models (LUTHER et al., 1988). In the short-wave component of ICRCCM (FOUQUART et al., 1991) two line-by-line models were used but their results were different mainly because of differences in the spectral intervals used. No agreement was then achieved on a standard reference.

More recent ICRCCM short wave results were analized by Barker et al. (2003). Short-wave codes used in nineteen institutions of nine countries were then compared. The reference results used in that study were obtained with the combination of LBLRTM — Line-By-Line Radiative Transfer Model, (CLOUGH et al., 1992) — and CHARTS, — Code for High-resolution Accelerated Radiative Transfer with Scattering, (MONCET; CLOUGH, 1997) — both developed at AER (Atmospheric and Environmental Researc, Inc., United States). According to Barker et al. (2003) it is safe to consider LBLRTM+CHARTS as the current modeling standard for clear-sky short-wave transfer. Eli Mlawer, Karen Cady-Pereira and Jennifer Delamere, of AER, provided to CPTEC some LBLRTM+CHARTS reference results for short-wave cases which were used for the comparisons reported here.

In the following discussion, CPTEC-old refers to the code which was operational into CPTEC's AGCM until March 2004 and whose climatology was described by Cavalcanti et al. (2002). CPTEC-new refers to the code which is operational since then (CHAGAS et al., 2004). CLIRAD refers to the code of Chou e Suarez (1999) as modified by Tarasova e Fomin (2000), also incorporated into CPTEC's AGCM (TARASOVA et al., 2007).

3.1 Gaseous extinction

Table 3.1 shows the main characteristics of the clear-sky (no clouds, no aerosols) cases used for the comparisons, where only gaseous absorption by atmospheric gases are taken into account. Cases `tro00`, `tro60` and `tro75`, reference cases used by Barker et al. (2003), are based on the year 2000 edition of the spectroscopic database HITRAN (ROTHMAN et al., 2003) and use the water vapor continuum formulation MT_CKD (MLAWER et al., 2004). Case `mls00`, provided by AER personnel, uses HITRAN 2004 (ROTHMAN et al., 2005) and MT_CKD.

TABLE 3.1 - Cases used for comparisons under clear (no clouds) and clean (no aerosols) conditions. TRO: tropical atmosphere, MLS: mid-latitude summer atmosphere.

Case	Profile	Solar zenith angle (^{o})	Surface albedo
tro00	TRO	0,0	0,2
tro60	TRO	59,9730	0,2
tro75	TRO	75,4629	0,2
mls00	MLS	0,0	0,2

Reference calculations have taken into account the main atmospheric short wave absorbers (H_2O, CO_2, O_3 and O_2) and also minor contributors (N_2O, CO and CH_4), using HITRAN 2004 and MT_CKD. According to Chou e Suarez (1999) the original CLIRAD takes into account H_2O, CO_2 and O_2, using HITRAN 1996 (ROTHMAN et al., 1998), and O_3, using absorption coefficients from WORLD METEOROLOGICAL ORGANIZATION (1986). The modified version of CLIRAD incorporated into CPTEC's AGCM have used the parameters of Tarasova e Fomin (2000) for H_2O and includes the water vapor continuum CKD (CLOUGH et al., 1989). The UKMO calculations have included absorption by H_2O, CO_2, O_3 and O_2, using HITRAN 2000 and version 2.4, released in 2002, of CKD. All reference fluxes presented here were integrated over the spectral band between 0.2 μm and 12.2 μm, and the solar flux over that interval, 1368.2 Wm^{-2}, was used as input for the broad-band codes.

3.1.1 Broad band comparisons

This section can be skipped while keeping the sequence. It is included for the sake of completeness as it displays detailed information which has lead to the summary presented in section 3.1.2. Tables 3.2, 3.3, 3.4 and 3.5 organize detailed results of the four clear-sky cases. The first part of each table displays values of short wave incident and reflected at top-of-atmosphere, absorbed by atmosphere and absorbed by surface. Reference values obtained with LBLRTM+CHARTS and with each broad-band code are shown. Explicit information on differences is also shown. The second part of each table exibits the same information as the first part but as partition fractions of incident short wave radiation instead of flux units. The essential results of the four tables are gathered in table 3.6.

3.1.2 Summary of clear sky cases

Table 3.6 summarizes the results of clear-sky cases.

TABLE 3.2 - **Case tro00.** Short wave radiation (in W/m^2) incident (InTA) and reflected (ReTA) at top-of-atmosphere, absorbed by atmosphere (AbAtm) and absorbed by surface (AbSfc), and corresponding partition fractions (α_p = ReTA/InTA, α_{atm} = AbAtm/InTA e α_{sfc} = AbSfc/InTA) for tropical atmosphere, solar zenith angle 0.0 degreee and surface albedo 0.2.

	LBLRTM	CPT-old		CPT-new		CLIRAD		UKMO	
				Fluxes(W/m^2):					
InTA	1368,16	1368,16	(0,00)	1368,16	(0,00)	1368,16	(0,00)	1368,16	(0,00)
ReTA	233,16	241,47	(+8,31)	236,84	(+3,68)	237,67	(+4,51)	231,98	(–1,18)
AbAtm	283,79	231,23	(–52,56)	250,96	(–32,83)	266,40	(–17,39)	275,39	(–8,40)
AbSfc	851,21	895,46	(+44,25)	880,36	(+29,15)	864,09	(+12,88)	860,79	(+9,58)
				Partition fractions:					
α_p	0,1704	0,1765	(+0,0061)	0,1731	(+0,0027)	0,1737	(+0,0033)	0,1696	(–0,0008)
α_{atm}	0,2074	0,1690	(–0,0384)	0,1834	(–0,0240)	0,1947	(–0,0127)	0,2013	(–0,0061)
α_{sfc}	0,6222	0,6545	(+0,0323)	0,6435	(+0,0213)	0,6316	(+0,0094)	0,6292	(+0,0070)

TABLE 3.3 - **Case tro60.** Short wave radiation (in W/m^2) incident (InTA) and reflected (ReTA) at top-of-atmosphere, absorbed by atmosphere (AbAtm) and absorbed by surface (AbSfc), and corresponding partition fractions (α_p = ReTA/InTA, α_{atm} = AbAtm/InTA e α_{sfc} = AbSfc/InTA) for tropical atmosphere, solar zenith angle 59.973 degreee and surface albedo 0.2.

	LBLRTM	CPT-old		CPT-new		CLIRAD		UKMO	
				Fluxes(W/m^2):					
InTA	684,64	684,64	(0,00)	684,64	(0,00)	684,64	(0,00)	684,64	(0,00)
ReTA	129,58	134,49	(+4,91)	131,87	(+2,38)	132,25	(+2,67)	127,81	(–1,77)
AbAtm	168,74	137,28	(–31,46)	148,26	(–20,48)	157,47	(–11,27)	162,52	(–6,22)
AbSfc	386,32	412,86	(+26,54)	404,51	(+18,19)	394,92	(+8,60)	394,30	(+7,98)
				Partition fractions:					
α_p	0,1893	0,1964	(+0,0071)	0,1926	(+0,0033)	0,1932	(+0,0039)	0,1867	(–0,0026)
α_{atm}	0,2465	0,2005	(–0,0460)	0,2166	(–0,0299)	0,2300	(–0,0165)	0,2374	(–0,0091)
α_{sfc}	0,5643	0,6030	(+0,0387)	0,5908	(+0,0265)	0,5768	(+0,0125)	0,5759	(+0,0116)

TABLE 3.4 - **Case tro75.** Short wave radiation (in W/m^2) incident (InTA) and reflected (ReTA) at top-of-atmosphere, absorbed by atmosphere (AbAtm) and absorbed by surface (AbSfc), and corresponding partition fractions (α_p = ReTA/InTA, α_{atm} = AbAtm/InTA e α_{sfc} = AbSfc/InTA) for tropical atmosphere, solar zenith angle 75.4629 degreee and surface albedo 0.2.

	LBLRTM	CPT-old		CPT-new		CLIRAD		UKMO	
				Fluxes(W/m^2):					
InTA	343,42	343,42	(0,00)	343,42	(0,00)	343,42	(0,00)	343,42	(0,00)
ReTA	74,00	77,86	(+3,86)	76,29	(+2,29)	75,83	(+1,83)	72,42	(–1,58)
AbAtm	100,32	81,47	(–18,85)	88,47	(–11,85)	93,77	(–6,55)	96,03	(–4,29)
AbSfc	169,10	184,08	(+14,98)	178,66	(+9,56)	173,82	(+4,72)	174,97	(+5,87)
				Partition fractions:					
α_p	0,2155	0,2267	(+0,0122)	0,2222	(+0,0067)	0,2208	(+0,0053)	0,2109	(–0,0046)
α_{atm}	0,2921	0,2372	(–0,0549)	0,2576	(–0,0345)	0,2730	(–0,0191)	0,2796	(–0,0125)
α_{sfc}	0,4924	0,5360	(+0,0436)	0,5202	(+0,0278)	0,5061	(+0,0137)	0,5095	(+0,0171)

In the following, the expression "code ***a*** is better than code ***b***" means that the results obtained by using code ***a*** are closer to the reference results than those obtained by using code ***b***. The main conclusions on the comparison of different short wave partition terms as a result of Table 3.6 figures are as follows.

Top-of-atmosphere reflectance. For overhead sun, top-of-atmosphere reflectance is overestimated by CPTEC-old, has its difference halved with CPTEC-new and CLIRAD,

TABLE 3.5 - **Case mls00.** Short wave radiation (in W/m^2) incident (InTA) and reflected (ReTA) at top-of-atmosphere, absorbed by atmosphere (AbAtm) and absorbed by surface (AbSfc), and corresponding partition fractions (α_p = ReTA/InTA, α_{atm} = AbAtm/InTA e α_{sfc} = AbSfc/InTA) for mid-latitude summer atmosphere, solar zenith angle 0.0 degreee and surface albedo 0.2.

	LBLRTM	CPT-old		CPT-new		CLIRAD		UKMO	
				Fluxes(W/m^2):					
InTA	1368,16	1368,16	(0,00)	1368,16	(0,00)	1368,16	(0,00)	1368,16	(0,00)
ReTA	236,13	242,94	(+6,81)	238,79	(+2,66)	240,34	(+4,21)	235,77	(–0,36)
AbAtm	264,84	219,13	(–45,71)	238,50	(–26,34)	251,56	(–13,28)	258,51	(–6,33)
AbSfc	867,19	906,08	(+38,89)	890,87	+23,68)	876,26	(+9,07)	873,88	(+6,69)
				Partition fractions:					
α_p	0,1726	0,1776	(+0,0050)	0,1745	(+0,0019)	0,1757	(+0,0031)	0,1723	(–0,0003)
α_{atm}	0,1936	0,1602	(–0,0334)	0,1743	(–0,0193)	0,1839	(–0,0097)	0,1889	(–0,0047)
α_{sfc}	0,6338	0,6623	(+0,0285)	0,6511	(+0,0173)	0,6405	(+0,0067)	0,6387	(+0,0049)

TABLE 3.6 - Partition of incident short-wave radiation (among reflected at top-of-atmosphere, absorbed by atmosphere and absorbed by surface) for clear-sky cases. Line-by-line LBLRTM+CHARTS results are shown in the second column; figures for broad-band codes CPT-old, CPT-new, CLIRAD and UKMO are differences of their results from line-by-line; cases are as described in Table 3.1.

Case	LBLRTM	CPT-old	CPT-new	CLIRAD	UKMO
		Top-of-atmosphere reflectance:			
tro00	0,170	+0,006	+0,003	+0,003	–0,001
mls00	0,173	+0,005	+0,002	+0,003	–0,000
tro60	0,189	+0,007	+0,003	+0,004	–0,003
tro75	0,216	+0,011	+0,007	+0,005	–0,005
		Atmosphere absorptance:			
tro00	0,207	–0,038	–0,024	–0,013	–0,006
mls00	0,194	–0,033	–0,019	–0,010	–0,005
tro60	0,247	–0,046	–0,030	–0,017	–0,009
tro75	0,292	–0,055	–0,035	–0,019	–0,013
		Surface absoptance:			
tro00	0,622	+0,032	+0,021	+0,009	+0,007
mls00	0,634	+0,029	+0,017	+0,007	+0,005
tro60	0,564	+0,039	+0,027	+0,013	+0,012
tro75	0,492	+0,044	+0,028	+0,014	+0,017

and is slightly underestimated by UKMO. Increasing the solar zenith angle, differences increase for all codes and CLIRAD's and UKMO's became comparable in magnitude but with opposite signal. In summary, CLIRAD is slightly better than CPTEC-new in calculating top-of-atmosphere reflectance, and UKMO is better than CLIRAD.

Atmosphere absorptance. For overhead sun, atmosphere absorptance is underestimated by CPTEC-old, has such a difference reduced with CPTEC-new, more reduced with CLIRAD, and even more with UMKO, which halves CLIRAD's differences. Increasing the solar zenith angle, differences increase proportionally for the four codes. In summary, CLIRAD is better than CPTEC-new in calculating atmosphere absorptance and UKMO is better than CLIRAD.

Surface absorptance. For overhead sun, surface absorptance is overestimated by CPTEC-old, this difference is reduced with CPTEC-new, halved with CLIRAD, and a bit more reduced with UKMO. Increasing the solar zenith angle, differences increase for the four codes. CLIRAD differences keep about half of CPTEC-new's differences but UKMO's differences grow quicker and become slightly bigger than CLIRAD's for large zenith angles. In summary, CLIRAD is better than CPTEC-new in evaluating surface absorptance, and UKMO is slightly better than CLIRAD for small zenith angles and slightly worse for large zenith angles.

3.2 Extinction by clouds

Cases with cloud are described in detail by Barker et al. (2003), who consider separately two overcast clouds, one at high and other at low altitude, and perform calculations with each one for three different solar zenith angles, then resulting six cases. Table 3.7 shows the main characteristics of these cases.

TABLE 3.7 - Cases used for comparisons under cloudy conditions. For all cases: tropical atmosphere, surface albedo 0.2 and overcast sky with clouds of liquid droplets of effective radius of 10 μm.

Case	Solar zenith angle (^{o})	base–top (km)	mixing ratio (g/kg)
high00	0,0	10,5–11,0	0,034
high60	59,9730	10,5–11,0	0,034
high75	75,4629	10,5–11,0	0,034
low00	0,0	3,5–4,0	0,159
low60	59,9730	3,5–4,0	0,159
low75	75,4629	3,5–4,0	0,159

CPTEC-old and CPTEC-new use as input the cloud cover fraction and combine it with other variables to estimate cloud optical thickness. CLIRAD also needs as input, apart from the cloud cover fraction, the effective radius of cloud particles (droplets or ice crystals) and, in CPTEC's implementation, adopts one fixed value for liquid water and another one for ice. In the results shown here, a value of 10 μm was used following the reference calculations. UKMO, apart from the cloud cover fraction and the effective radius, also requires as input the mixing ratio of condensed water and the ratio between ice and liquid water amounts (ice fraction) within the cloud. As the current cloud scheme of CPTEC's AGCM only parametrizes the cloud cover fraction, it was necessary to incorporate a cloud microphysics scheme to generate the other parameteres. The cloud microphysics scheme of the CCM3 (KIEHL et al., 1998) was then implemented (see section 5.2). In obtaining the results presented here, a fixed effective radius of 10 μm, mixing ratio values from Table 3.7 and a ice fraction of zero were used to conform to reference calculations.

3.2.1 High cloud

Like what was said about section 3.1.1 this section can be skipped too. Tables 3.8, 3.9 and 3.10 display detailed information which is summarized in table 3.14 used for analysis.

TABLE 3.8 - **Case high00.** Short wave radiation (in W/m^2) incident (InTA) and reflected (ReTA) at top-of-atmosphere, absorbed by atmosphere (AbAtm) and absorbed by surface (AbSfc), and corresponding partition fractions (α_p = ReTA/InTA, α_{atm} = AbAtm/InTA e α_{sfc} = AbSfc/InTA) for tropical atmosphere, solar zenith angle 0.0 degreee, surface albedo 0.2 and an overcast cloud between 10.5 and 11.0 km.

	LBLRTM	CPT-old		CPT-new		CLIRAD		UKMO	
				Fluxos(W/m^2):					
InTA	1368,16	1368,16	(0,00)	1368,16	(0,00)	1368,16	(0,00)	1368,16	(0,00)
ReTA	256,95	247,94	(–9,01)	243,36	(–13,59)	249,97	(–6,98)	258,17	(+1,22)
AbAtm	287,81	231,45	(–56,36)	251,23	(–36,58)	267,64	(–20,17)	280,35	(–7,46)
AbSfc	823,40	888,76	(+65,36)	873,56	(+50,16)	850,54	(+27,14)	829,64	(+6,24)
				Frações de partição:					
α_p	0,1878	0,1812	(–0,0066)	0,1779	(–0,0099)	0,1827	(–0,0051)	0,1887	(+0,0009)
α_{atm}	0,2104	0,1692	(–0,0412)	0,1836	(–0,0268)	0,1956	(–0,0148)	0,2049	(–0,0055)
α_{sfc}	0,6018	0,6496	(+0,0478)	0,6385	(+0,0367)	0,6217	(+0,0199)	0,6064	(+0,0046)

TABLE 3.9 - **Case high60.** Short wave radiation (in W/m^2) incident (InTA) and reflected (ReTA) at top-of-atmosphere, absorbed by atmosphere (AbAtm) and absorbed by surface (AbSfc), and corresponding partition fractions (α_p = ReTA/InTA, α_{atm} = AbAtm/InTA e α_{sfc} = AbSfc/InTA) for tropical atmosphere, solar zenith angle 59.973 degreee, surface albedo 0.2 and an overcast cloud between 10.5 and 11.0 km.

	LBLRTM	CPT-old		CPT-new		CLIRAD		UKMO	
				Fluxos(W/m^2):					
InTA	684,64	684,64	(0,00)	684,64	(0,00)	684,64	(0,00)	684,64	(0,00)
ReTA	197,24	170,55	(–26,69)	167,95	(–29,29)	164,28	(–32,96)	186,38	(–10,86)
AbAtm	153,91	129,50	(–24,41)	139,94	(–13,97)	149,28	(–4,63)	149,15	(–4,76)
AbSfc	333,49	384,59	(+51,10)	376,75	(+43,26)	371,08	(+37,59)	349,11	(+15,62)
				Frações de partição:					
α_p	0,2881	0,2491	(–0,0390)	0,2453	(–0,0428)	0,2399	(–0,0482)	0,2722	(–0,0159)
α_{atm}	0,2248	0,1892	(–0,0356)	0,2044	(–0,0204)	0,2180	(–0,0068)	0,2179	(–0,0069)
α_{sfc}	0,4871	0,5617	(+0,0746)	0,5503	(+0,0632)	0,5420	(+0,0549)	0,5099	(+0,0228)

3.2.2 Low cloud

This section also can be skipped. Tables 3.11, 3.12 and 3.13 display detailed information which is summarized in table 3.14 used for analysis.

TABLE 3.10 - **Case high75.** Short wave radiation (in W/m^2) incident (InTA) and reflected (ReTA) at top-of-atmosphere, absorbed by atmosphere (AbAtm) and absorbed by surface (AbSfc), and corresponding partition fractions (α_p = ReTA/InTA, α_{atm} = AbAtm/InTA e α_{sfc} = AbSfc/InTA) for tropical atmosphere, solar zenith angle 75.4629 degreee, surface albedo 0.2 and an overcast cloud between 10.5 and 11.0 km.

	LBLRTM	CPT-old		CPT-new		CLIRAD		UKMO	
				Fluxos(W/m^2):					
InTA	343,42	343,42	(0,00)	343,42	(0,00)	343,42	(0,00)	343,42	(0,00)
ReTA	146,04	116,48	(–29,56)	114,96	(–31,08)	110,25	(–35,79)	129,61	(–16,43)
AbAtm	72,95	69,29	(–3,66)	75,09	(+2,14)	80,11	(+7,16)	74,44	(+1,49)
AbSfc	124,43	157,64	(+33,21)	153,37	(+28,94)	153,06	(+28,63)	139,37	(+14,94)
				Frações de partição:					
α_p	0,4253	0,3392	(–0,0861)	0,3347	(–0,0906)	0,3210	(–0,1043)	0,3774	(–0,0479)
α_{atm}	0,2124	0,2018	(–0,0106)	0,2187	(+0,0063)	0,2333	(+0,0209)	0,2167	(+0,0043)
α_{sfc}	0,3623	0,4590	(+0,0967)	0,4466	(+0,0843)	0,4457	(+0,0834)	0,4058	(+0,0435)

TABLE 3.11 - **Case low00.** Short wave radiation (in W/m^2) incident (InTA) and reflected (ReTA) at top-of-atmosphere, absorbed by atmosphere (AbAtm) and absorbed by surface (AbSfc), and corresponding partition fractions (α_p = ReTA/InTA, α_{atm} = AbAtm/InTA e α_{sfc} = AbSfc/InTA) for tropical atmosphere, solar zenith angle 0.0 degreee, surface albedo 0.2 and an overcast cloud between 3.5 and 4.0 km.

	LBLRTM	CPT-old		CPT-new		CLIRAD		UKMO	
				Fluxes(W/m^2):					
InTA	1368,16	1368,16	(0,00)	1368,16	(0,00)	1368,16	(0,00)	1368,16	(0,00)
ReTA	529,78	294,42	(–235,36)	289,24	(–240,54)	291,67	(–238,11)	517,10	(–12,68)
AbAtm	307,72	242,37	(–65,35)	262,62	(–45,10)	278,22	(–29,50)	300,59	(–7,13)
AbSfc	530,66	831,37	(+300,71)	816,30	(+285,64)	798,27	(+267,61)	550,48	(+19,82)
				Partition fractions:					
α_p	0,3872	0,2152	(–0,1720)	0,2114	(–0,1758)	0,2132	(–0,1740)	0,3779	(–0,0093)
α_{atm}	0,2249	0,1772	(–0,0477)	0,1919	(–0,0330)	0,2034	(–0,0215)	0,2197	(–0,0052)
α_{sfc}	0,3879	0,6077	(+0,2198)	0,5966	(+0,2087)	0,5835	(+0,1956)	0,4023	(+0,0144)

3.2.3 Summary of cases with clouds

Similarly to the clear-sky cases, comparative analyses and conclusions will be based on table 3.14. Nevertheless it is worth bringing to attention a remarkable pattern present in the three cases with low clouds (tables 3.11, 3.12 and 3.13): errors in short wave reflected at top-of-atmosphere and absorbed by surface calculated by CPTEC-old, CPTEC-new and CLIRAD are very large. For the short wave reflected at top-of-atmosphere, errors of CPTEC-old and CPTEC-new vary between 23 and 45 % of reference values and errors of CLIRAD range from 26 to 45 %, while for UKMO the erros are between 1.6 and 2.4 %. For the short wave absorbed by surface, errors of CPTEC-old and CPTEC-new vary between 54 and 89 % of reference values and errors of CLIRAD range from 50 to 84 %, while for UKMO the erros are between 3.7 and 13 %.

Cloudy-sky cases are summarized in table 3.14, from which some conclusions can be drawn on the different terms of short wave partition as calculated by the different codes.

Top-of-atmosphere reflectance. High cloud: for the four codes, errors increase with

TABLE 3.12 - **Case low60.** Short wave radiation (in W/m^2) incident (InTA) and reflected (ReTA) at top-of-atmosphere, absorbed by atmosphere (AbAtm) and absorbed by surface (AbSfc), and corresponding partition fractions (α_p = ReTA/InTA, α_{atm} = AbAtm/InTA e α_{sfc} = AbSfc/InTA) for tropical atmosphere, solar zenith angle 59.973 degreee, surface albedo 0.2 and an overcast cloud between 3.5 and 4.0 km.

	LBLRTM	CPT-old		CPT-new		CLIRAD		UKMO	
				Fluxes(W/m^2):					
InTA	684,64	684,64	(0,00)	684,64	(0,00)	684,64	(0,00)	684,64	(0,00)
ReTA	350,14	229,19	(–120,95)	225,43	(–124,71)	221,05	(–129,09)	344,09	(–6,05)
AbAtm	155,65	131,04	(–24,61)	141,48	(–14,17)	149,19	(–6,46)	148,53	(–7,12)
AbSfc	178,85	324,41	(+145,56)	317,73	(+138,88)	314,41	(+135,56)	192,02	(+13,17)
				Partition fractions:					
α_p	0,5114	0,3348	(–0,1766)	0,3293	(–0,1821)	0,3229	(–0,1885)	0,5026	(–0,0088)
α_{atm}	0,2274	0,1914	(–0,0360)	0,2067	(–0,0207)	0,2179	(–0,0095)	0,2169	(–0,0105)
α_{sfc}	0,2612	0,4738	(+0,2126)	0,4641	(+0,2029)	0,4592	(+0,1980)	0,2805	(+0,0193)

TABLE 3.13 - **Case low75.** Short wave radiation (in W/m^2) incident (InTA) and reflected (ReTA) at top-of-atmosphere, absorbed by atmosphere (AbAtm) and absorbed by surface (AbSfc), and corresponding partition fractions (α_p = ReTA/InTA, α_{atm} = AbAtm/InTA e α_{sfc} = AbSfc/InTA) for tropical atmosphere, solar zenith angle 75.4629 degreee, surface albedo 0.2 and an overcast cloud between 3.5 and 4.0 km.

	LBLRTM	CPT-old		CPT-new		CLIRAD		UKMO	
				Fluxes(W/m^2):					
InTA	343,42	343,42	(0,00)	343,42	(0,00)	343,42	(0,00)	343,42	(0,00)
ReTA	194,83	149,64	(–45,19)	147,01	(–47,82)	144,00	(–50,83)	191.81	(–3,02)
AbAtm	83,07	69,73	(–13,34)	75,19	(–7,88)	78,82	(–4,25)	77,51	(–5,56)
AbSfc	65,52	124,04	(+58,52)	121,21	(+55,69)	120,60	(+55,08)	74,10	(+8,58)
				Partition fractions:					
α_p	0,5673	0,4357	(–0,1316)	0,4281	(–0,1392)	0,4193	(–0,1480)	0,5585	(–0,0088)
α_{atm}	0,2419	0,2031	(–0,0388)	0,2190	(–0,0229)	0,2295	(–0,0124)	0,2257	(–0,0162)
α_{sfc}	0,1908	0,3612	(+0,1704)	0,3530	(+0,1622)	0,3512	(+0,1604)	0,2158	(+0,0250)

solar zenith angle; errors of CPTEC-old, CPTEC-new and CLIRAD are of the same order, with CLIRAD's a bit larger than others'; errors of UKMO are lees than half of CLIRAD's. Low cloud: again the errors of CPTEC-old, CPTEC-new and CLIRAD are of the same order, but now they do not vary to much with solar zenith angle; errors of UKMO do not vary with solar zenith angle and are much smaller than the other codes' errors, being about 5 to 6 % of CLIRAD's errors. Summary: UKMO is better than others for high cloud and much better for low cloud.

Atmosphere absorptance. High cloud: for solar zenith angles 0^o and 60^o, CLIRAD and UKMO have similar errors and are better than CPTEC-old and CPTEC-new; for large solar zenith angles, UKMO is better than CLIRAD. Low cloud: for overhead sun, CLIRAD is better than CPTEC-old and CPTEC-new and UKMO is better than CLIRAD; for large solar zenith angles, CLIRAD is better than CPTEC-old and CPTEC-new and slightly better than UKMO. Summary: in average, UKMO is a little better than CLIRAD.

Surface absorptance. High cloud: for the four codes, errors increase with solar zenith an-

TABLE 3.14 - Partition of incident short-wave radiation (among reflected at top-of-atmosphere, absorbed by atmosphere and absorbed by surface) for cloudy-sky cases. Line-by-line LBLRTM+CHARTS results are shown in the second column; figures for broad-band codes CPT-old, CPT-new, CLIRAD and UKMO are differences of their results from line-by-line; cases are as described in Table 3.7.

Case	LBLRTM	CPT-old	CPT-new	CLIRAD	UKMO
		Top-of-atmosphere reflectance:			
high00	0,188	–0,007	–0,010	–0,005	+0,001
high60	0,288	–0,039	–0,043	–0,048	–0,016
high75	0,425	–0,086	–0,091	–0,104	–0,048
low00	0,387	–0,172	–0,176	–0,174	–0,009
low60	0,511	–0,177	–0,182	–0,189	–0,009
low75	0,567	–0,132	–0,139	–0,148	–0,009
		Atmosphere absorptance:			
high00	0,210	–0,041	–0,027	–0,015	–0,006
high60	0,225	–0,036	–0,020	–0,007	–0,007
high75	0,212	–0,011	+0,006	+0,021	+0,004
low00	0,225	–0,048	–0,033	–0,022	–0,005
low60	0,227	–0,036	–0,021	–0,010	–0,011
low75	0,242	–0,039	–0,023	–0,012	–0,016
		Surface absorptance:			
high00	0,602	+0,048	+0,037	+0,020	+0,005
high60	0,487	+0,075	+0,063	+0,055	+0,023
high75	0,362	+0,097	+0,084	+0,083	+0,044
low00	0,388	+0,220	+0,209	+0,196	+0,014
low60	0,261	+0,213	+0,203	+0,198	+0,019
low75	0,191	+0,170	+0,162	+0,160	+0,025

gle; errors decrease following the order CPTEC-old, CPTEC-new, CLIRAD and UKMO; errors of UKMO reach a little more than half of CLIRAD's errors. Low cloud: errors have a slight decrease from CPTEC-old to CPTEC-new and to CLIRAD; errors of UKMO are much smaller, about 10 % of CLIRAD's. Summary: UKMO is better for high cloud and much better for low cloud.

3.3 Extinction by aerosols

The codes CPTEC-old and CPTEC-new are not prepared to calculate the extinction by aerosols. CLIRAD is prepared for that but single scattering properties of aerosols (optical thickness, single scattering albedo and asymmetry) need to be specified as input for each layer and spectral band in order to calculate the extinction. UKMO code provides parametrizations for 13 aerosol types in the spectral file currently in use at CPTEC. Absorption coefficient, single scattering albedo and asymmetry, for each absorption band, are available for 9 aerosol types (*water soluble, dust-like, oceanic, soot, sulphuric acid, fresh soot, aged soot, biomass 1, biomass 2*) and the same parameters, for each absorption band and for 21 relative humidity values (the boundaries of the twenty 0.05-wide intervals between 0 and 1) are available for 4 types (*accumulation mode sulphate, Aitken mode sulphate, NaCl film mode, NaCl jet mode*). To obtain the total aerosol optical thickness it is neceesary to feed the code with the mixing ratios of each aerosol type in each grid box of the model.

At the moment, along with the incorporation of UKMO code, a simplified aerosol climatology according to Cusack et al. (1998) was implemented into CPTEC's AGCM (see section 5.3). UKMO's aerosol parametrization has not been tested here in off-line mode but the simplified climatology was included in the long-term runs analized in Chapters 6 and 7.

3.4 Concluding remarks

The off-line comparisons discussed here, which take into account short-wave extinction by atmospheric gases and clouds, lead to some basic conclusions. The main conclusion of section 3.1 is that UKMO code is the best of the four codes compared to simulate short-wave fluxes for clear and clean sky conditions. The main conclusion of section 3.2 is that UKMO code is better than the others to simulate short-wave fluxes when high thin clouds are present and incomparably better in the presence of thick low clouds. The main conclusion of section 3.3 is that UKMO is able to parametrize short-wave extinction by aerosols from the concentration of different aerosol species, while CLIRAD includes aerosol extinction only if single scattering properties of aerosols are provided and CPTEC is unable to calculate aerosol extinction.

4 OFF-LINE COMPARISONS OF LONG-WAVE CODES

Prior to the incorporation of UKMO-LW into the AGCM, current CPTEC long-wave code and UKMO-LW were compared in off-line mode. Cases for comparison were taken from the long-wave component of ICRCCM program (ELLINGSON et al., 1991). The following sections show selected results for cases 25 to 34, summarized in Table 4.1. Detailed description of atmospheric profiles and gaseous absorbers considered in each case can be found in Ellingson et al. (1991).

4.1 Cooling rate profiles

Figures 4.1 and 4.2 show the long-wave cooling-rate profiles obtained when using current operational long-wave code of CPTEC's AGCM and UKMO-LW. As benchmark references, results of line-by-line calculations of Fomin e Gershanov (1996) and LBLRTM results taken from Robert Ellingson's "Longwave ICRCCM page" (http://www.met.fsu.edu/people/ellingson/LBLWeb/) are also plotted.

The main message of these figures: differences in the cooling rate profiles are small.

4.2 Long wave fluxes

Figure 4.3 compares the net long-wave fluxes at the surface as calculated by current long-wave code of CPTEC's AGCM and by UKMO-LW for the cases described in Table 4.1. Figure 4.4 does analogous comparison for the upward long-wave fluxes at the top of atmosphere. Three reference results are plotted in these figures: the line-by-line results of Fomin e Gershanov (1996) and the average and one standard deviation limits of the results of Ellingson et al. (1991), contributed from an average of 36 different codes, for the ten cases, and LBLRTM results for six cases.

TABLE 4.1 - Cases from Ellingson et al. (1991) used for comparison between different long-wave codes.

Case number	H_2O and O_3 profiles	CO_2 concentration (ppmv)
25	Tropical - TRO	300
26	Tropical - TRO	600
27	Mid-latitude summer - MLS	300
28	Mid-latitude summer - MLS	600
29	Mid-latitude winter - MLW	300
30	Mid-latitude winter - MLW	600
31	Subarctic summer - SAS	300
32	Subarctic summer - SAS	600
33	Subarctic winter - SAW	300
34	Subarctic winter - SAW	600

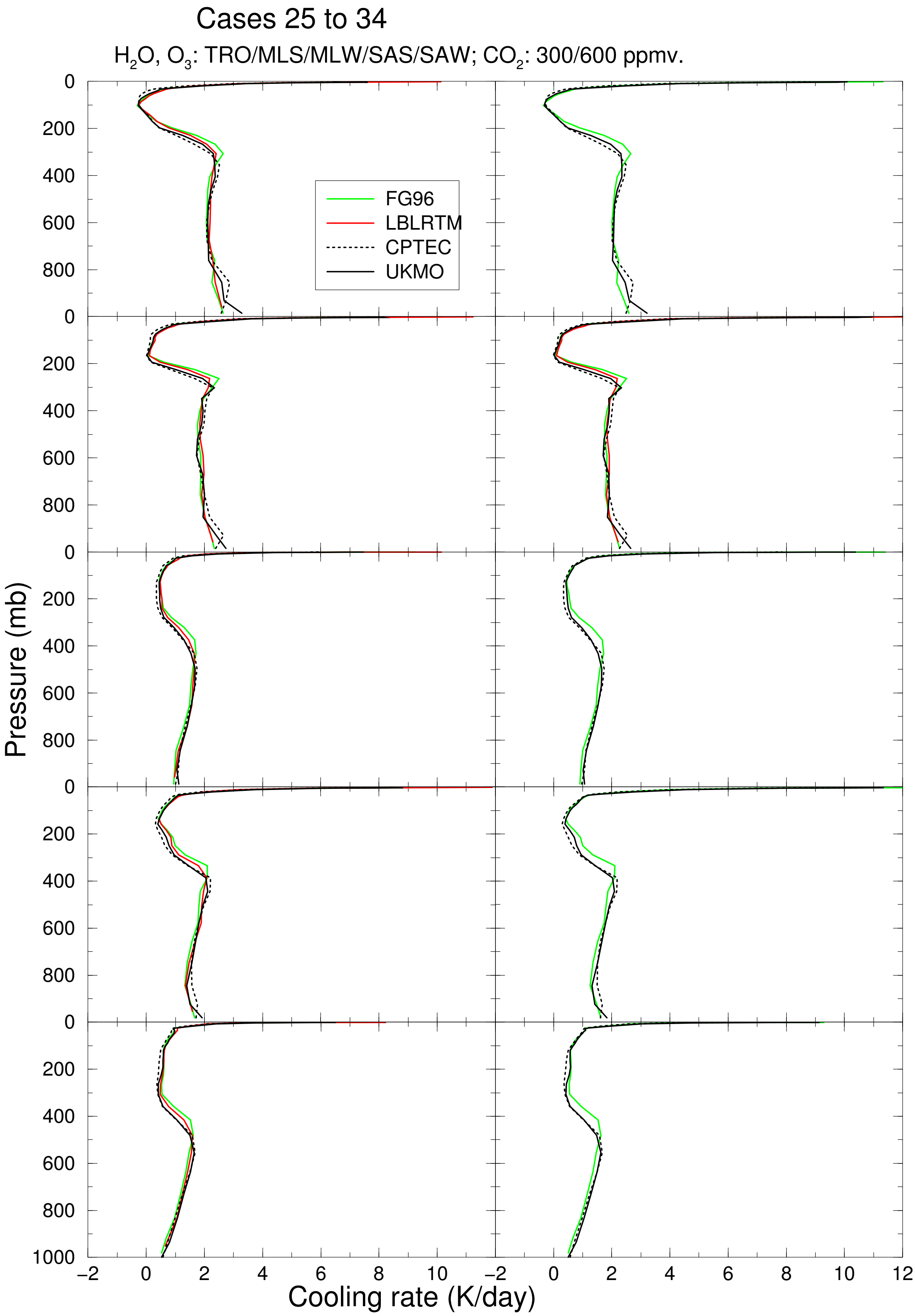

FIGURE 4.1 - Long-wave cooling-rate profiles calculated by current operational code of CPTEC's AGCM, by UKMO-LW code, and by line-by-line code (FOMIN; GERSHANOV, 1996), for cases 25 to 34 of Ellingson et al. (1991) as described in Table 4.1. LBLRTM profiles for some cases are also plotted. First column, from top to bottom, displays results of cases 25, 27, 29, 31, and 33; second column, from top to bottom, displays results of cases 26, 28, 30, 32, and 34.

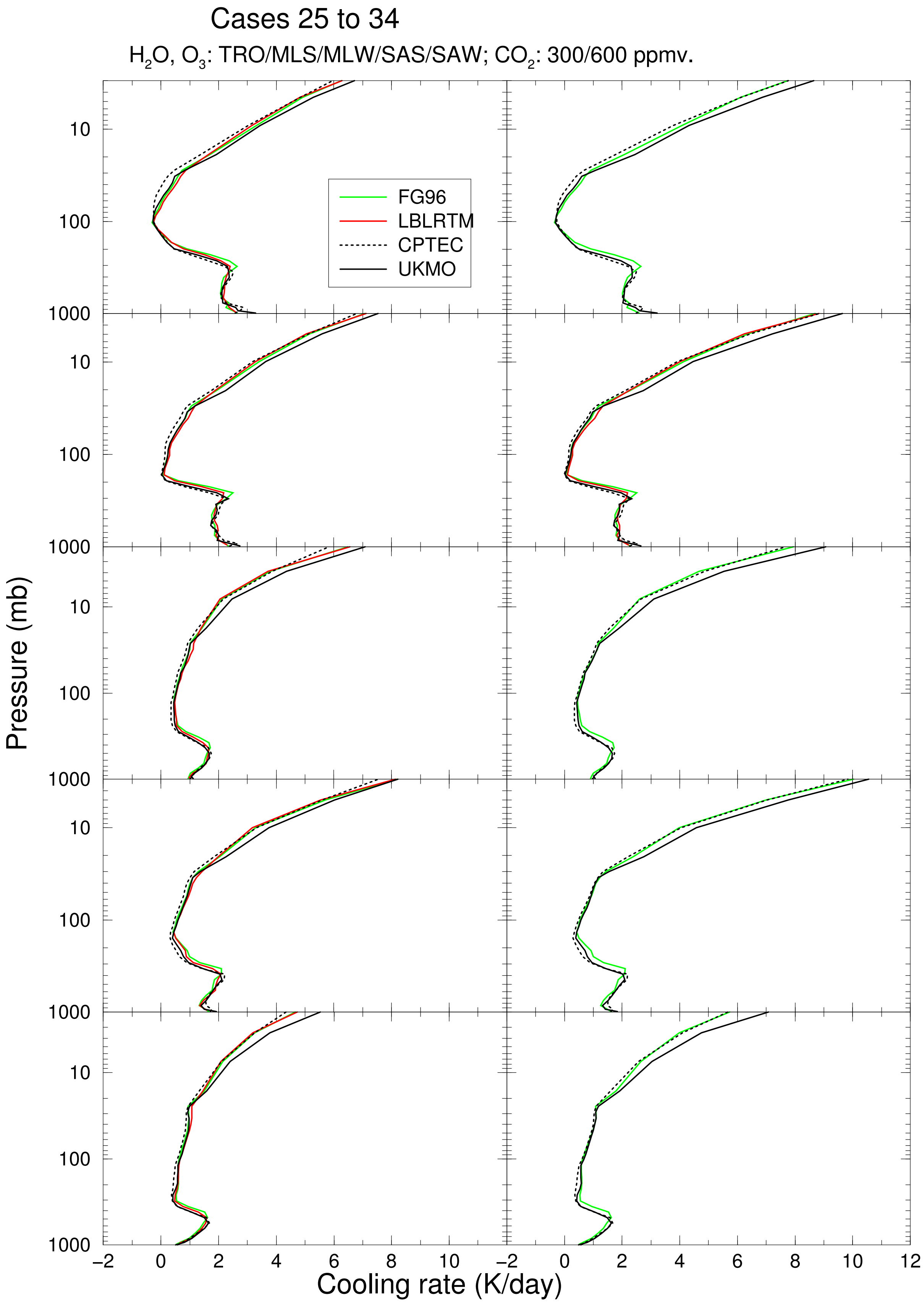

FIGURE 4.2 - Same as Figure 4.1, except that pressure axis is logaritmic instead of linear.

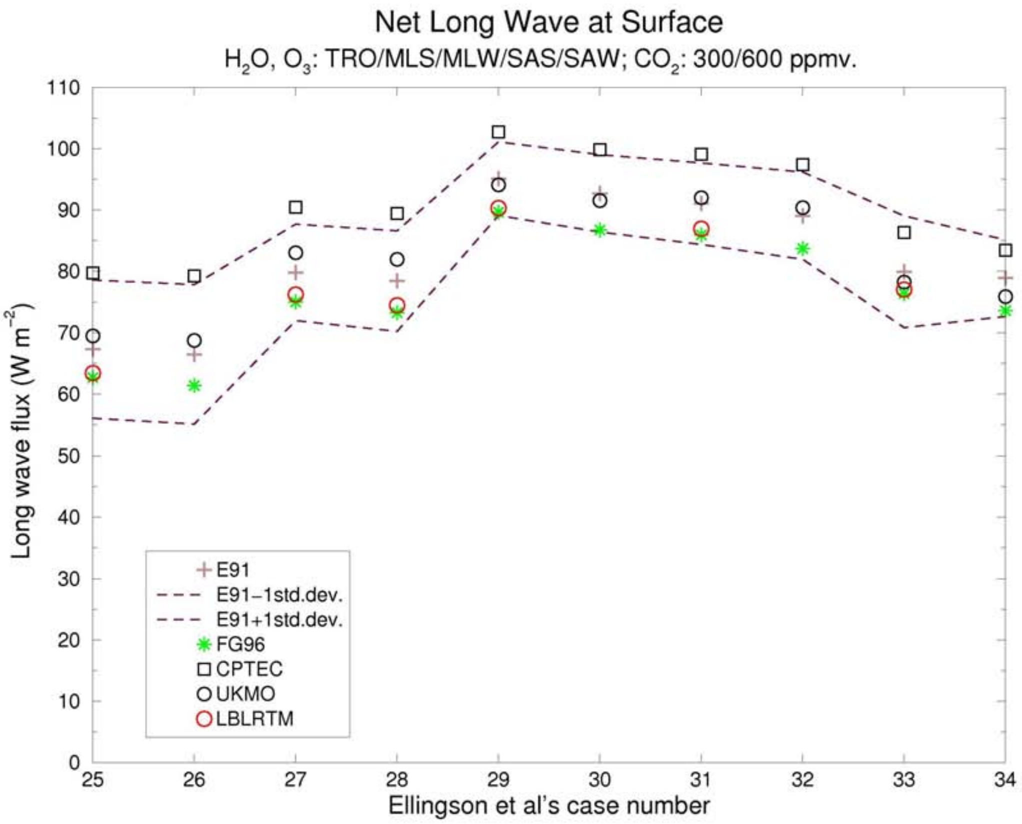

FIGURE 4.3 - Net long wave fluxes at the surface calculated by current operational code of CPTEC's AGCM and by UKMO-LW code for cases 25 to 34 of Ellingson et al. (1991) as described in Table 4.1 . Pluses (+) and dashed lines represent the average and one standard deviation limits of results from an average of 36 different codes; stars represent the line-by-line results of Fomin e Gershanov (1996); red circles represent LBLRTM results.

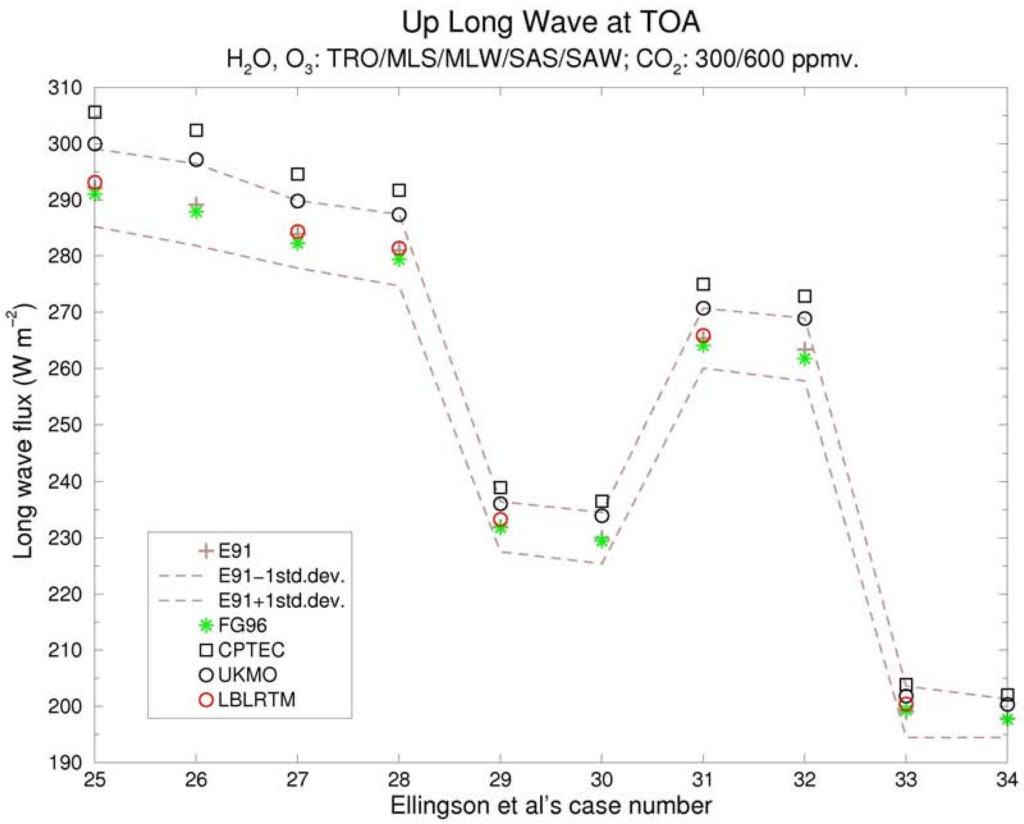

FIGURE 4.4 - Upward long wave fluxes at the top of atmosphere calculated by current operational code of CPTEC's AGCM and by UKMO-LW code for cases 25 to 34 of Ellingson et al. (1991) as described in Table 4.1 . Pluses (+) and dashed lines represent the average and one standard deviation limits of results from an average of 36 different codes; stars represent the line-by-line results of Fomin e Gershanov (1996); red circles represent LBLRTM results.

It can be seen that UKMO-LW sistematically brings the long-wave fluxes closer to the reference values as compared to the current CPTEC's long-wave code, specially for the upward long-wave fluxes at the top of atmosphere.

5 INCORPORATION INTO CPTEC'S AGCM

5.1 Overview

Inside the module `PhysicsDriver` of CPTEC's AGCM, subroutine `DryPhysics` calls subroutine `physcs` which in turn calls subroutine `spmrad`. Subroutine `spmrad`, part of module `Radiation`, is the main subroutine for radiation parameterization.

Main **input** for `spmrad` is:

call interval for short wave routine,
call interval for long wave routine,
surface pressure,
surface temperature,
visible diffuse surface albedo,
near-infrared diffuse surface albedo,
visible beam surface albedo,
near-infrared beam surface albedo,
temperature profile,
specific humidity profile,
relative humidity profile,
vertical velocity profile,
profile of sigma coordinate at bottom of each layer and
profile of sigma coordinate at middle of each layer.

Main **output** of `spmrad` is:

profile of cooling rate due to long wave radiation,
profile of heating rate due to short wave radiation,
upward long wave flux at top of atmosphere (all-sky and clear),
downward short wave flux at top of atmosphere (all-sky and clear),
downward long wave flux at bottom of atmosphere (all-sky and clear),
net long wave flux at surface (all-sky and clear),
downward visible diffuse flux at surface (all-sky and clear),
downward near-infrared diffuse flux at surface (all-sky and clear),
downward visible beam flux at surface (all-sky and clear) and
downward near-infrared beam flux at surface (all-sky and clear).

The structure of `spmrad` subroutine was kept as described in Chagas e Tarasova (1996) where different subroutines, `swrad` and `lwrad`, were called at different time-steps for computing short-wave and long-wave fluxes. In the UKMO code however, there is only one main radiation routine `radiance_calc` which can be used for computing short-wave or long-wave radiances or fluxes. Hence, for being able to call the UKMO scheme for both short wave and long wave, an interface `MODULE` was written. This module is called `UKMO_Intf` and contains subroutines to initialize the UKMO scheme, i.e., to read the spectral file, to prepare the aerosol climatology, to configure the short-wave and long-wave calls, and to call `radiance_calc` to calculate either short-wave or long-wave fluxes. These subroutines are named `ukmo_swintf` and `ukmo_lwintf` respectivelly and are called from `spmrad`. Input and output arguments are described in the code and are basically the same as the original `swrad` and `lwrad` plus information on aerosols and cloud microphysics.

5.2 Clouds

For evaluating fluxes and heating rates, UKMO's code requires cloud micro-physics parameters which are not calculated within CPTEC's AGCM as they are not necessary for current radiation code. A calculation of these parameters was included based on the methods used in the NCAR Community Climate Model CCM3 (KIEHL et al., 1996).

5.2.1 Condensate mixing ratio

The vertical profile of water concentration inside the clouds is assumed to have an exponential decay given by:

$$\rho_l = \rho_l^0 \exp\left(-z/h_l\right), \tag{5.1}$$

where $\rho_l^0 = 0.21 g/m^3$. The height scale for liquid water, h_l, is a diagnostic variable calculated from the vertically integrated water vapor content (precipitable water):

$$h_l = 700 \ln \left[1 + \frac{1}{g}\int_{p_T}^{p_{sfc}} q dp\right] \tag{5.2}$$

where h_l is obtained in meters and p_T and p_{sfc} are top-of-atmosphere and surface pressure respectively. The cloud water path, cwp, is determined by integrating the liquid water concentration:

$$cwp = \int \rho_l dz \tag{5.3}$$

and, for each model layer, it can be calculated analitically as

$$cwp(k) = \rho_l^0 h_l \left[\exp(-z_{bot(k)}/h_l) - \exp(-z_{top(k)}/h_l)\right] \tag{5.4}$$

where cwp is given in g/m^2 and z_{bot} and z_{top} are respectively the heights of the base an top of the k^{th} layer.

To obtain the condensed water mixing ratio in each layer, first the *dry air path (dap)* is calculated using the hydrostatic equation:

$$dap(k) = \int \rho_{air} dz = \frac{\Delta p(k)}{g} \tag{5.5}$$

And the mixing ratio is given by:

$$lmixr(k) \quad = \quad \frac{cwp(k)}{dap(k)} = g\frac{cwp(k)}{\Delta p(k)}10^{-5} \tag{5.6}$$

where cwp is calculated from equation 5.4 in g/m^2 and Δp is given in $mbar$. The factor 10^{-5} comes from unit transformation from $mbar$ to Pa and from kg/m^2 to g/m^2.

5.2.2 Effective radius

Observations had shown that there is a big difference between droplets' effective size r_e for continental and maritime warm clouds. Because of that and following CCM3 (KIEHL, 1994), the effective radius for liquid water clouds (r_{el}) over the ocean is taken as $10\mu m$ and over the continent is given by:

$$r_{el} = \begin{cases} 5\mu m & T > -10°C \\ 5 - 5(T+10)/20\mu m & -30°C <= T <= -10°C \\ r_{ei} & T < -30°C \end{cases} \tag{5.7}$$

The effective radius of ice crystals, r_{ei}, is diagnosed from the ratio between level pressure and surface pressure, being constant in sigma levels:

$$r_{ei} = \begin{cases} 10\mu m & \sigma > \sigma^{high} \\ r_{ei}^{min} - (r_{ei}^{max} - r_{ei}^{min}) \left[\frac{\sigma - \sigma^{high}}{\sigma^{high} - \sigma^{low}}\right] & \sigma <= \sigma^{high} \end{cases} \tag{5.8}$$

where $r_{ei}^{max} = 30\mu m$, $r_{ei}^{min} = 10\mu m$, $\sigma^{high} = 0.4$ e $\sigma^{low} = 0.0$. The behaviour of functions $r_{el}(T)$ and $r_{ei}(\sigma)$ is shown in Figure 5.1.

5.2.3 Cloud cover and ice fraction

Cloud cover fraction is calculated by subroutine `cldgen` inside module `Radiation`. Stratiform clous are generated by `cldgen` in three distinct levels,—high, medium and low—following the work of Slingo (1987). In each layer two cloud types only—convective ($clu(k)$) e stratiform ($cld(k)$)—are provided. It is assumed that a fraction of the liquid water con-

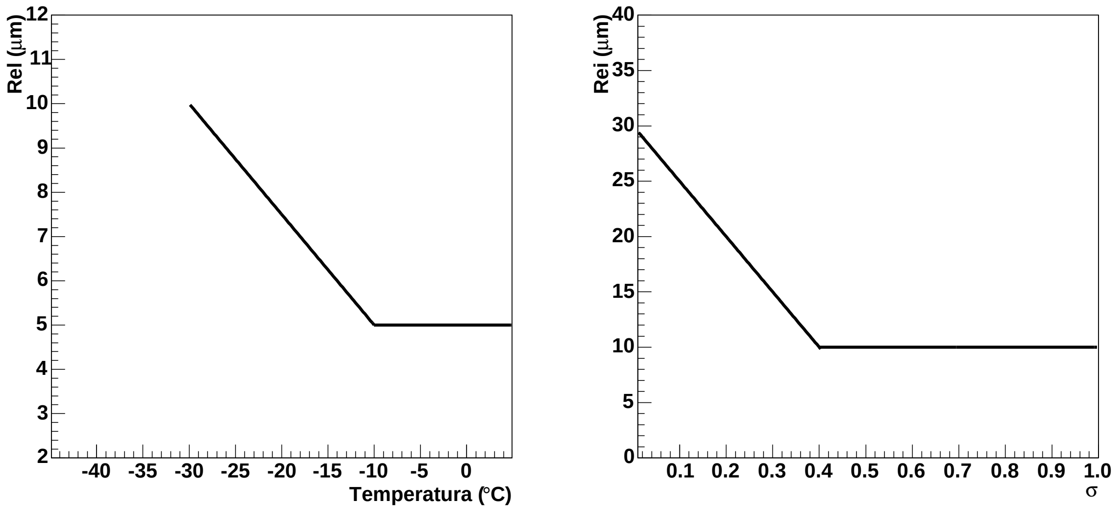

FIGURE 5.1 - Effective radius for droplets (left) and ice crystals (right) according to the parametrization of Kiehl (1994).

tent is in the form of ice crystals, depending on layer temperature. For temperatures above $-10°C$ there is only liquid and below $-30°C$ there is only ice. A mixed phase is considered between these temperatures and the ice fraciton is given by:

$$f_{ice} = \begin{cases} 0 & T > -10°C \\ -(T+10)/20 & -30°C <= T <= -10°C \\ 1 & T < -30°C \end{cases} \tag{5.9}$$

A curve of ice fraction as a function of temperature is shown in Figure 5.2.

As a result, four cloud types are provided as input to the UKMO radiation code and their characteristics are as follow:

a) Convective water cloud:

- Effective radius = $rel(k)$
- Mixing ratio = $lmixr(k) * (1 - f_{ice}(k))$
- Cloud cover fraction = $clu(k) * (1 - f_{ice}(k))$

b) Convective ice cloud:

- Effective radius = $rei(k)$
- Mixing ratio = $lmixr(k) * f_{ice}(k)$
- Cloud cover fraction = $clu(k) * f_{ice}(k)$

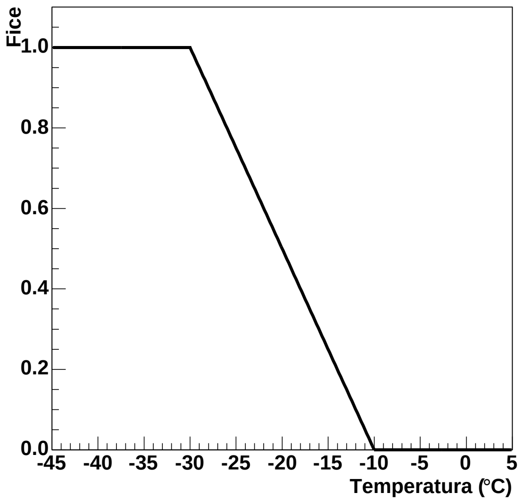

FIGURE 5.2 - Fraction of cloud condensed water which is as ice crystals as a function of layer temperature.

c) Stratiform water cloud:

- Effective radius $= rel(k)$
- Mixing ratio $= lmixr(k) * (1 - f_{ice}(k))$
- Cloud cover fraction $= cld(k) * (1 - f_{ice}(k))$

d) Stratiform ice cloud:

- Effective radius $= rei(k)$
- Mixing ratio $= lmixr(k) * f_{ice}(k)$
- Cloud cover fraction $= cld(k) * f_{ice}(k)$

In order to calculate the optical properties of a cloud type from these parameters there is still a need of the scattering properties of a single particle. These scattering properties depend on the spectral band and are read from the spectral file (EDWARDS; THELEN, 2003).

5.3 Aerosols

A simplified aerosol climatology was implemented as input for the UKMO radiation code following Cusack et al. (1998). Although simplified, it allows the introduction of first order effects of aerosols on the energy balance and achieves good agreement with observations.

The climatology used is as described in WORLD METEOROLOGICAL ORGANIZATION (1982), WORLD METEOROLOGICAL ORGANIZATION (1983) with minor changes. Two aerosol profiles, CONT-I and MAR-I, are used, MAR-I on grid points over the ocean or ice and CONT-I on grid points over land.

Each profile is divided in three distinct regions: boundary layer, troposphere and stratosphere. The aerosol mixture in each region is a combination of five basic aerosol types of WMO's climatology: *water-soluble*, *dust*, *soot*, *oceanic* and *stratospheric sulphates*. Refraction indices and size distributions for each component are given in WORLD METEOROLOGICAL ORGANIZATION (1983) and were used for obtaining the necessary optical properties—single scattering albedo, asymmetry factor and absorption coefficient—read directly from the spectral file.

Moreover, mixing ratios are needed as input for the code. Table 5.1 shows the amount of each aerosol type in each atmospheric region from which mixing ratios are calculated. To

TABLE 5.1 - Composition of each atmospheric region as total column amounts ($aermass$) of each aerosol type given in kg/m^2. BL means boundary layer.

	water	dust	oceanic	soot	sulfur
BL Land	2.77579e-5	6.70018e-5	0.0	9.57169e-7	0.0
BL Ocean	1.07535e-5	0.0	2.043167e-4	0.0	0.0
Free Troposphere	3.46974e-6	8.37523e-6	0.0	1.19646e-7	0.0
Stratosphere	0.0	0.0	0.0	0.0	1.86604e-6

calculate mixing ratios from the data on Table 5.1 it is necessary to divide them by the total amount of air in each region:

$$airmass = \int \rho_{air} dz = \frac{p_{bot} - p_{top}}{g} \tag{5.10}$$

where p_{bot} and p_{top} are the region base and top pressure.

It is also necessary to apply a scale factor on all levels inside the troposphere to make sure that a smaller aerosol amount will be present over grid points above sea level (NAKAJIMA et al., 1996). This scale factor is given by $p_\star/p_\circ$, where $p_\star$ is the surface pressure and $p_\circ = 1.013 \times 10^5$ is the sea level pressure.

The mixing ratio, $mixr(j)$, of the j^{th} aerosol type is constant on each region and is calculated by dividing the values from Table 5.1 by Equation 5.10 and multiplying by the scale factor:

$$mixr(j) = \frac{aermass(j)}{airmass} \times \text{scale factor} \tag{5.11}$$

$$= aermass(j) \times \begin{cases} \frac{g}{p_{bot}-p_{top}} \frac{p_\star}{p_\circ} = \frac{g}{(\sigma_{bot}-\sigma_{top})p_\circ} & \text{boundary layer, troposphere} \\ \frac{g}{p_{bot}-p_{top}} = \frac{g}{(\sigma_{bot}-\sigma_{top})p_\star} & \text{stratosphere} \end{cases} \tag{5.12}$$

where σ_{bot} and σ_{top} are the sigma levels at base and top of the region. The mixing ratios calculated by previous equation, for continental and maritime profiles, are shown in Table 5.2.

The extinction coefficient due the aerosols in each layer is calculated as:

$$\tau_{aerosol}(k) = \sum_{j=water,...}^{sulfur} mixr(k,j) \times (A+S) \times \frac{\Delta p(k)}{g} \tag{5.13}$$

where $mixr(k,j)$ is the mixing ratio of the j^{th} aerosol type at the k^{th} level (Table 5.2), A and S are absorption and scattering coefficients (in m^2/kg) read from the spectral file and $\Delta p(k)/g$ is the air mass in the layer (in kg/m^2). Then:

$$\tau_{aer}(k) = \begin{cases} \frac{g}{(\sigma_{bot}-\sigma_{top})p_\circ} \times (A+S) \times \frac{\Delta p(k)}{g} = \frac{\Delta\sigma(k)}{1-\sigma_{BL}^{trop}}(A+S)\frac{p_\star}{p_\circ} & \text{boundary layer} \\ \frac{g}{(\sigma_{bot}-\sigma_{top})p_\circ} \times (A+S) \times \frac{\Delta p(k)}{g} = \frac{\Delta\sigma(k)}{\sigma_{BL}^{trop}-\sigma_{trop}^{strat}}(A+S)\frac{p_\star}{p_\circ} & \text{troposphere} \\ \frac{g}{(\sigma_{bot}-\sigma_{top})p_\star} \times (A+S) \times \frac{\Delta p(k)}{g} = \frac{\Delta\sigma(k)}{\sigma_{trop}^{strat}}(A+S) & \text{stratosphere} \end{cases} \tag{5.14}$$

TABLE 5.2 - Composition of the two aerosol profiles given as mixing ratios $mixr(k, j)$ of each one of the five aerosol types from the climatology. Figures are in 10^{-10} and , in the stratosphere, $p_\star$ was made equal to $p_\circ$.

	CONT-I					MAR-I				
P(mbar)	water	dust	oceanic	soot	sulfur	water	dust	oceanic	soot	sulfur
2.8	-	-	-	-	23.1	-	-	-	-	23.1
10.2	-	-	-	-	23.1	-	-	-	-	23.1
18.5	-	-	-	-	23.1	-	-	-	-	23.1
29.2	-	-	-	-	23.1	-	-	-	-	23.1
42.3	-	-	-	-	23.1	-	-	-	-	23.1
58.8	-	-	-	-	23.1	-	-	-	-	23.1
79.2	-	-	-	-	23.1	-	-	-	-	23.1
104.1	3.9	9.4	-	0.1	-	3.9	9.4	-	0.1	-
134.3	3.9	9.4	-	0.1	-	3.9	9.4	-	0.1	-
170.4	3.9	9.4	-	0.1	-	3.9	9.4	-	0.1	-
212.8	3.9	9.4	-	0.1	-	3.9	9.4	-	0.1	-
261.6	3.9	9.4	-	0.1	-	3.9	9.4	-	0.1	-
316.6	3.9	9.4	-	0.1	-	3.9	9.4	-	0.1	-
376.8	3.9	9.4	-	0.1	-	3.9	9.4	-	0.1	-
441.4	3.9	9.4	-	0.1	-	3.9	9.4	-	0.1	-
508.2	3.9	9.4	-	0.1	-	3.9	9.4	-	0.1	-
575.5	3.9	9.4	-	0.1	-	3.9	9.4	-	0.1	-
641.1	3.9	9.4	-	0.1	-	3.9	9.4	-	0.1	-
703.3	3.9	9.4	-	0.1	-	3.9	9.4	-	0.1	-
760.6	3.9	9.4	-	0.1	-	3.9	9.4	-	0.1	-
811.8	3.9	9.4	-	0.1	-	3.9	9.4	-	0.1	-
856.8	3.9	9.4	-	0.1	-	3.9	9.4	-	0.1	-
895.3	3.9	9.4	-	0.1	-	3.9	9.4	-	0.1	-
927.8	3.9	9.4	-	0.1	-	3.9	9.4	-	0.1	-
954.8	754.3	1821.0	-	26.0	-	292.2	-	5552.0	-	-
976.9	754.3	1821.0	-	26.0	-	292.2	-	5552.0	-	-
994.9	754.3	1821.0	-	26.0	-	292.2	-	5552.0	-	-
1007.9	754.3	1821.0	-	26.0	-	292.2	-	5552.0	-	-

6 LONG-TIME RUNS WITH UKMO SHORT-WAVE CODE

Part of the material presented and discussed in this chapter was presented at the "12th Conference on Atmospheric Radiation" held at Madison, Wisconsin, United States, in July 2006 (CHAGAS; BARBOSA, 2006). It describes the results of the first step of the incorporation of UKMO radiation code into CPTEC's AGCM, when only the short-wave code was replaced.

Two four-member-ensemble integrations of current CPTEC AGCM at T62L28 resolution were performed for ten years (1982 to 1991), one with current radiation code and other with UKMO short-wave code. Selected results are present below. Section 6.1 present grand figures of globally averaged annual means for the four ten-year integrations and Section 6.2 displays selected yearly-averaged fields.

6.1 Global means

Table 6.1 shows the annual global mean solar radiation absorbed at the top of atmosphere and its partition between atmosphere and surface for the two integrations. Also shown are climatological values for the old CPTEC code taken from Cavalcanti et al. (2002), mean observed values of NASA/GEWEX Surface Radiation Budget Project (WHITLOCK et al., 1993) for the same period, and multimodel means and standard deviations taken from Wild (2005) and Wild et al. (2006). Even though the results of Wild (2005) and Wild et al. (2006) refer to a different period of model integrations, it is instructive to take their values as representative of models' climatology worldwide.

TABLE 6.1 - Global mean solar radiation budgets (in Wm^{-2}) for CPTEC AGCM. CPTEC-old: original model with Davies (1982) formulation; CPTEC-new: current operational model with Ramaswamy e Freidenreich (1992) formulation; UKMO: current model with Edwards e Slingo (1996) short-wave code; Wild05 and Wild06: figures taken from Wild (2005) and Wild et al. (2006); SRB: NASA/GEWEX SRB dataset (WHITLOCK et al., 1993).

		Clear-sky			
	CPTEC-old	CPTEC-new	UKMO	Wild06	SRB
Top-of-atmosphere	296	298	290	288(2.4)	288
Atmosphere	57	62	74	69(6.7)	70
Surface	239	236	216	219(6.2)	218
		All-sky			
	CPTEC-old	CPTEC-new	UKMO	Wild05	SRB
Top-of-atmosphere	249	244	243	236(6.5)	241
Atmosphere	58	63	75	74(7.3)	74
Surface	191	181	168	162(8.4)	167

6.2 Annual means

Figures 6.1, 6.2 and 6.3 display fields of annual means of the clear-sky incident short-wave at the surface, of the all-sky incident short-wave at the surface, and of the short-wave budget at the surface for the NASA/GEWEX SRB Project, taken as reference, for the current CPTEC AGCM and for the CPTEC AGCM with the UKMO short-wave code, along with differences from reference.

Inspection on the figures of Table 6.1 reveals the successive improvements on the global mean solar radiation budgets when the old (prior to 2004) CPTEC code (DAVIES, 1982) was modified to the new CPTEC code (RAMASWAMY; FREIDENREICH, 1992) and when this last one was replaced by UKMO code (EDWARDS; SLINGO, 1996).

Figures 6.1, 6.2 and 6.3 clearly show how the annual mean of the clear-sky and all-sky incident shortwave at surface and the all-sky short-wave budget are much better represented by the CPTEC's AGCM with UKMO code than with current CPTEC code. As for all-sky, there are still big differences in some regions of the globe when UKMO is used, which are smaller but follow the same pattern as in CPTEC code. These differences are probably related to the cumulus convection and cloud schemes, not to the radiation scheme.

As for the impacts of the new short-wave code on other climatological fields, Figures 6.4 and 6.5 show that the impact on the cloud cover and precipitation fields are small.

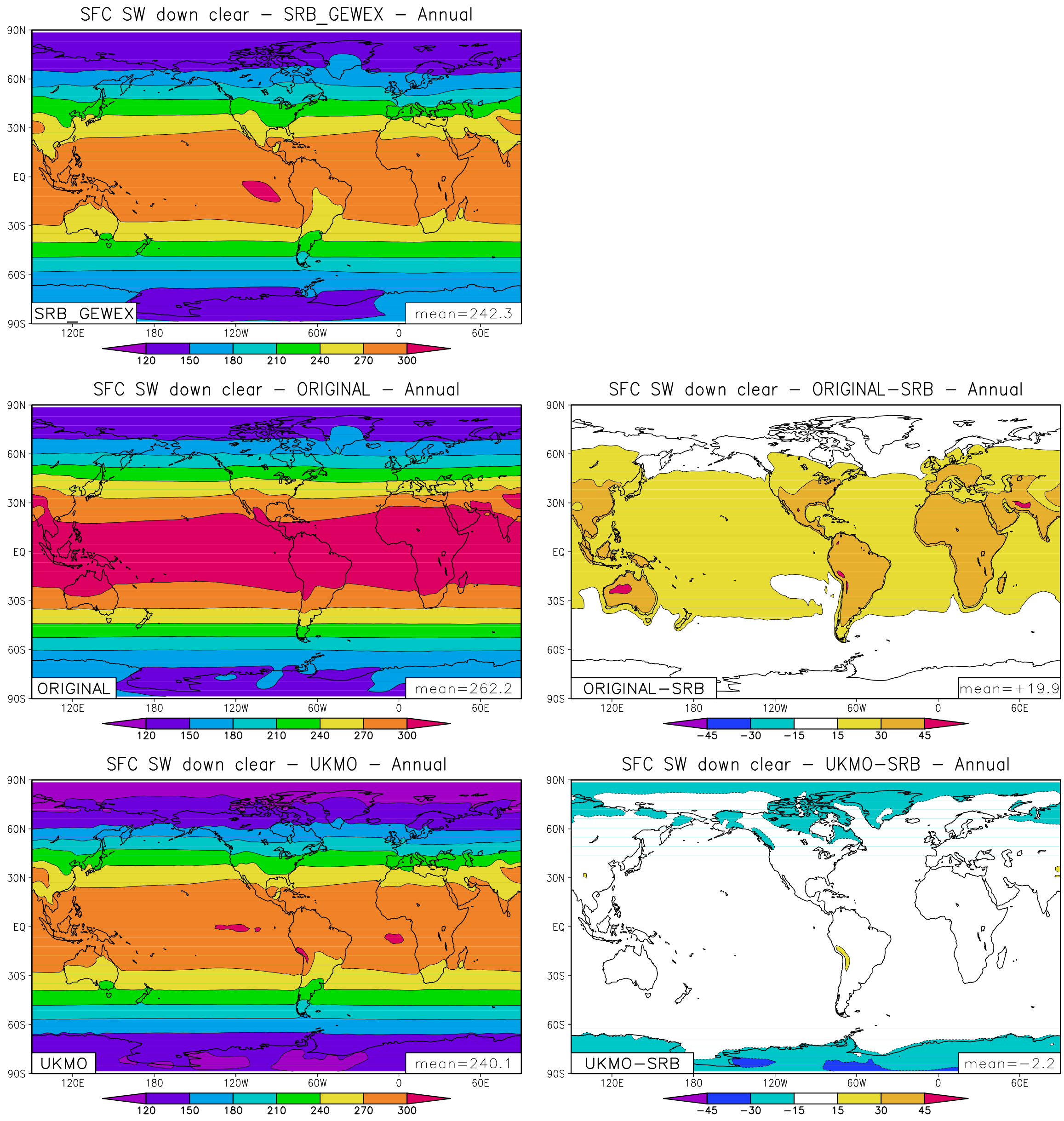

FIGURE 6.1 - Annual mean of the clear-sky incident short wave at the surface (Wm^{-2}). Top: generated by NASA/GEWEX SRB Project; middle: calculated by current CPTEC AGCM and difference from SRB; bottom: calculated by CPTEC AGCM with UKMO short-wave code and difference from SRB.

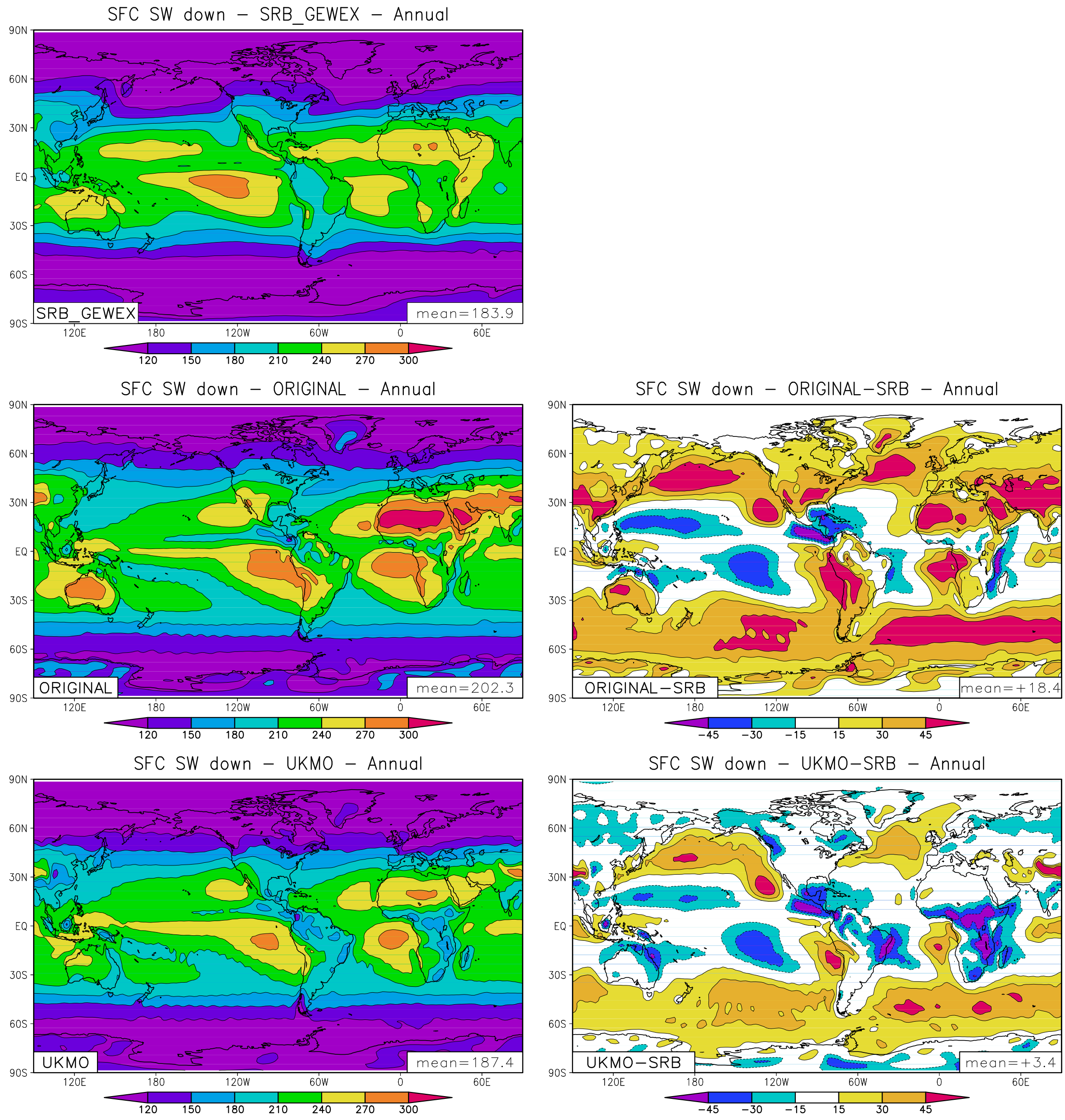

FIGURE 6.2 - Annual mean of the all-sky incident short wave at the surface (Wm^{-2}). Top: generated by NASA/GEWEX SRB Project; middle: calculated by current CPTEC AGCM and difference from SRB; bottom: calculated by CPTEC AGCM with UKMO short-wave code and difference from SRB.

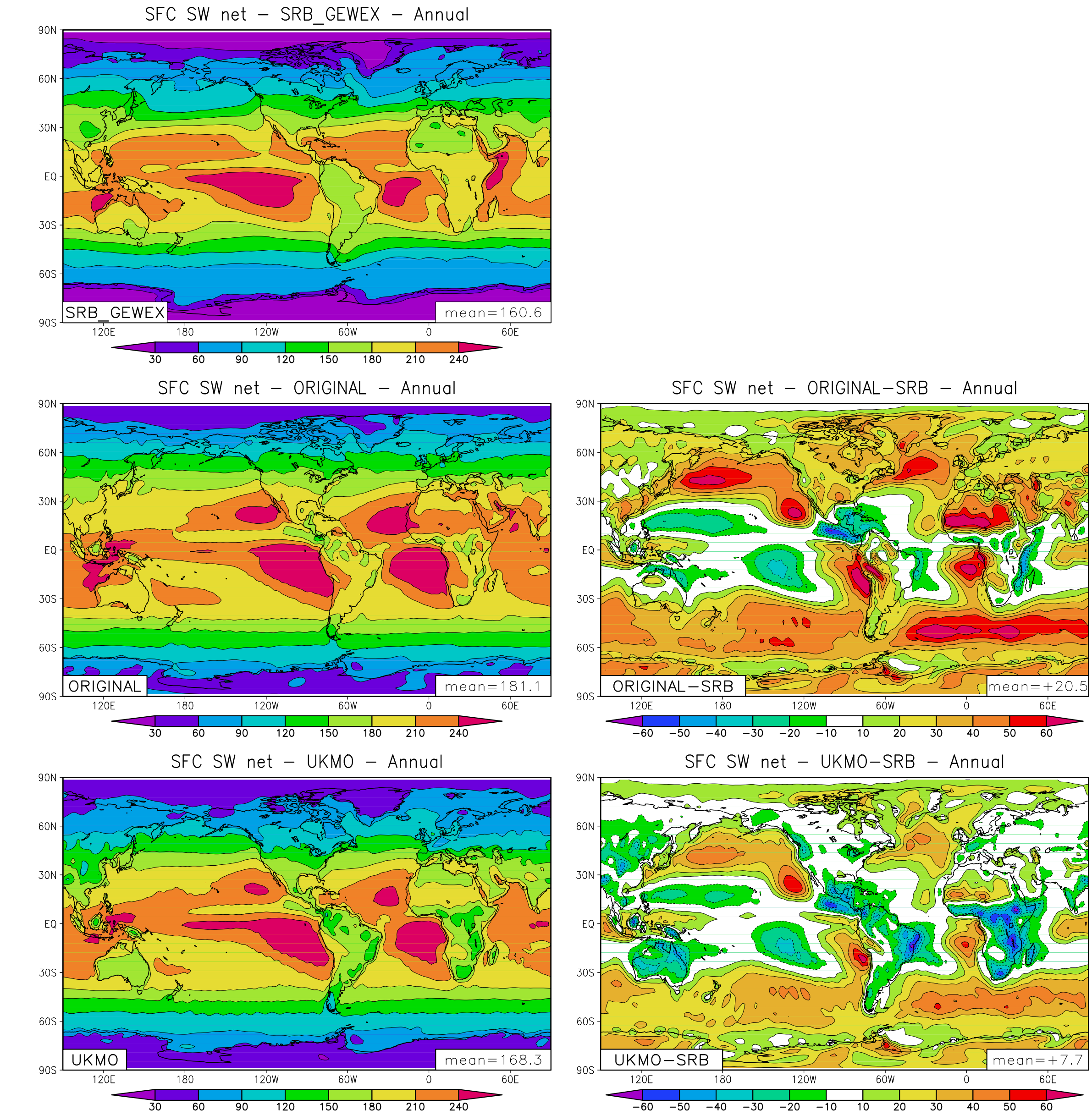

FIGURE 6.3 - Annual mean of the short-wave budget at the surface (Wm^{-2}). Top: generated by NASA/GEWEX SRB Project; middle: calculated by current CPTEC AGCM and difference from SRB; bottom: calculated by CPTEC AGCM with UKMO short-wave code and difference from SRB.

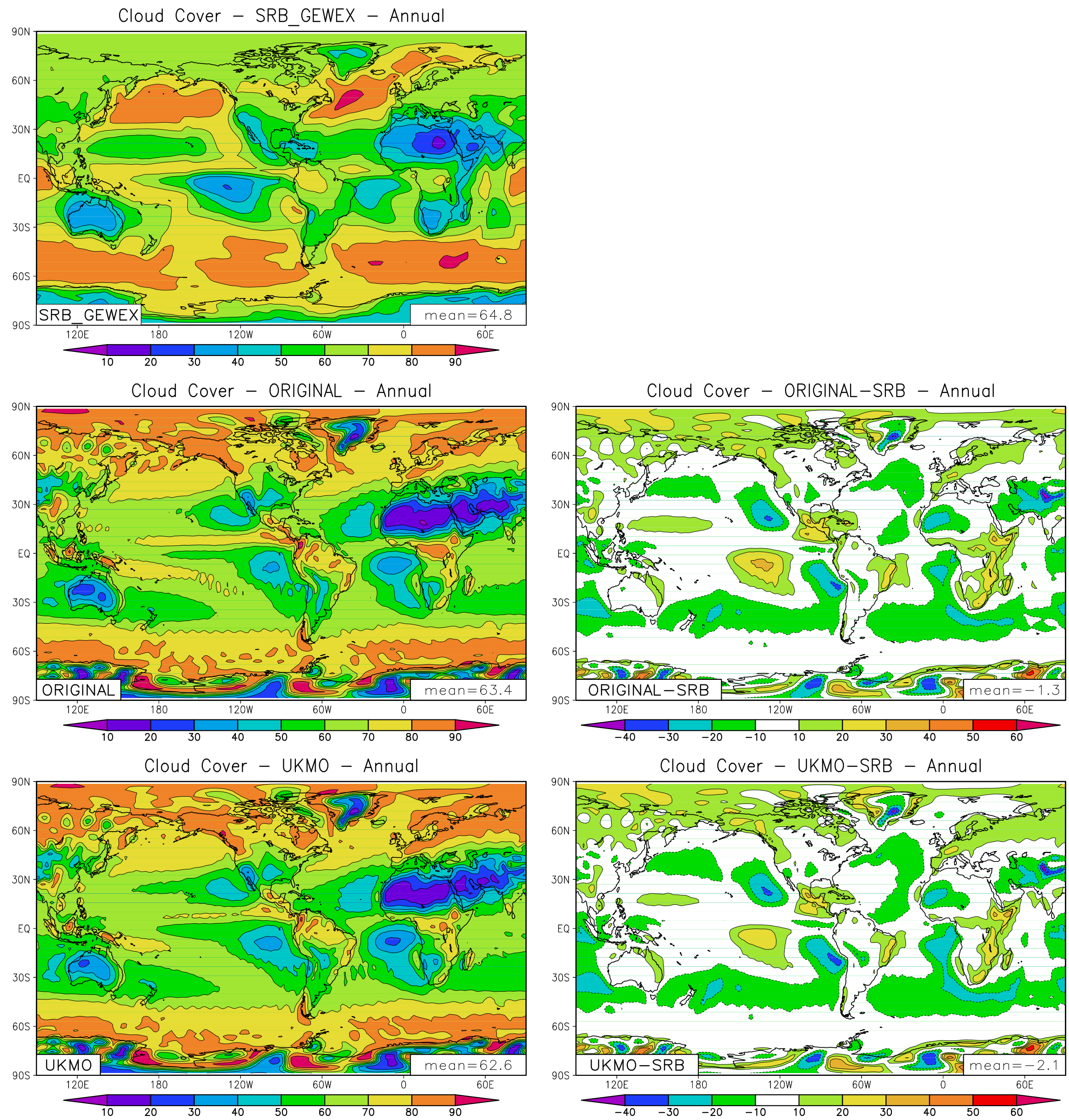

FIGURE 6.4 - Annual mean of cloud cover (in percent). Top: generated by NASA/GEWEX SRB Project; middle: calculated by current CPTEC AGCM and difference from SRB; bottom: calculated by CPTEC AGCM with UKMO short-wave code and difference from SRB.

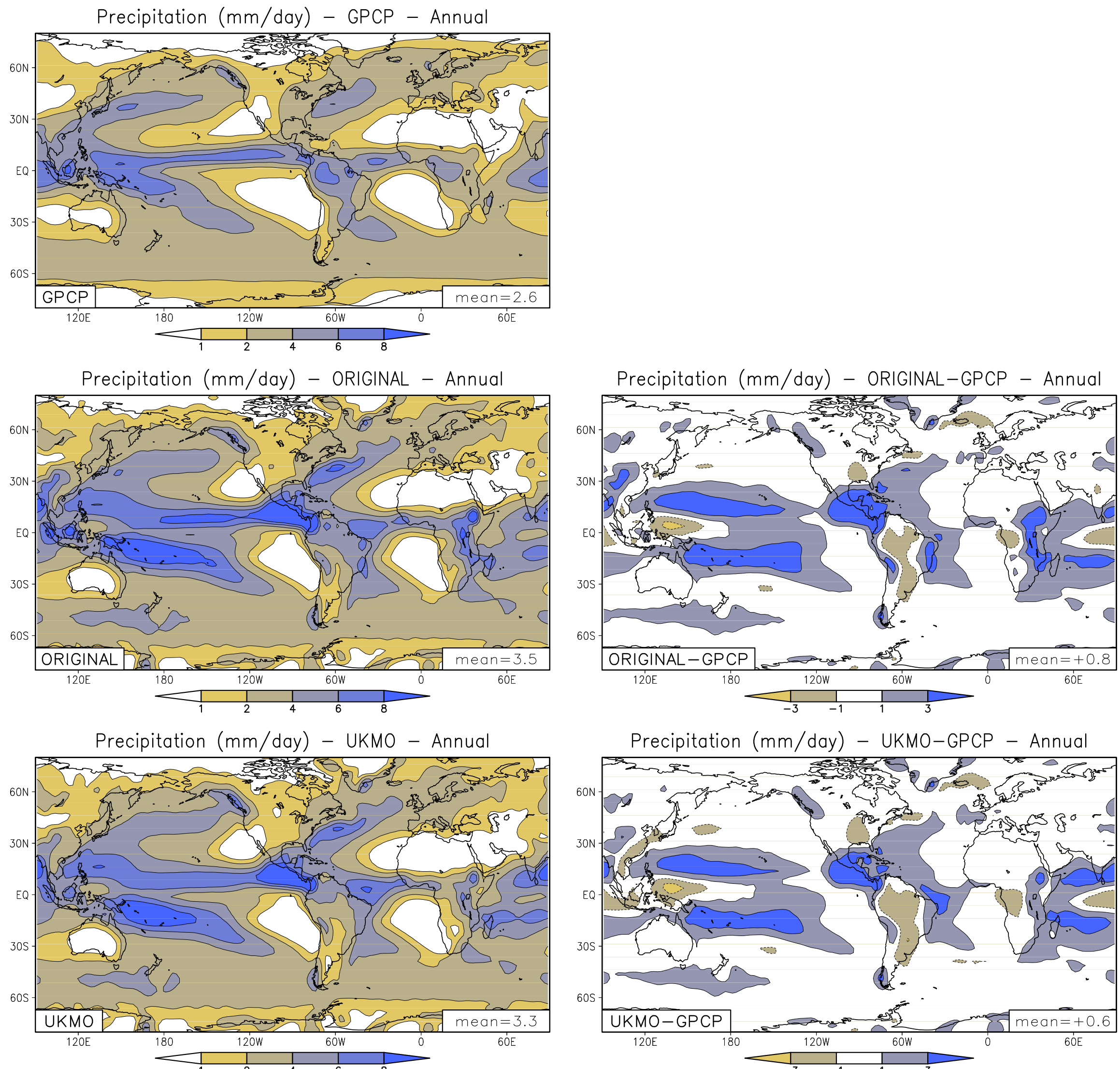

FIGURE 6.5 - Annual mean of the total precipitation (mm day^{-1}). Top: measured by GPCP Project; middle: calculated by current CPTEC AGCM and difference from GPCP; bottom: calculated by CPTEC AGCM with UKMO short-wave code and difference from GPCP.

7 LONG-TIME RUNS WITH UKMO CODE

This chapter compares mean fields obtained from long-term runs of CPTEC's AGCM with UKMO code for both short wave and long wave, and with current radiation code. It also shows results of runs with CLIRAD replacing current short-wave code. Part of the material presented and discussed here was presented at the "International Radiation Symposium 2008" held at Foz do Iguaçu, PR, Brazil, in August 2008 (CHAGAS; BARBOSA, 2008). In summary, three different versions of radiation parameterization were used:

a) Short-wave: current; long-wave: current. Referred to as CPTEC.

b) Short-wave: CLIRAD; long-wave: current. Referred to as CLIRAD.

c) Short-wave: UKMO; long-wave: UKMO. Referred to as UKMO.

For this preliminary analysis the three versions of the AGCM were integrated for a 13-month period starting in November 1st 2002. Results are displayed as one-year-averaged fields (December/2002—November/2003) and three-month-averaged fields for two periods (December/2002—February/2003 and June/2003—August/2003). The analysis will be focussed on the short-wave and long-wave fluxes at top-of-atmosphere and at surface.

7.1 Short-wave fluxes

The short-wave fluxes, as calculated by CPTEC, CLIRAD, and UKMO are compared with release 2.5 of the dataset produced by the NASA/GEWEX Surface Radiative Budget Project (SRB). Figures 7.1, 7.2, and 7.3 show respectively one-year-averaged global fields of 1) the incident short-wave all-sky flux at surface, 2) the incident clear-sky short-wave flux at surface, and 3) the net all-sky short-wave flux at surface. Every figure shows seven plots of the appropriate field, one from the SRB dataset, taken as reference, and the other three pairs displaying the results of the three AGCM runs along with the differences of these runs and the SRB reference. Global means of the twelve-month and three-month averaged short-wave radiative fluxes are summarized in Table 7.1.

Inspection on Table 7.1 allows some general conclusions for the grand figures (global annual averages) of short-wave fluxes: incident short-wave at surface is badly modeled by CPTEC for both clear-sky and all-sky; for clear-sky, the lack of more than 20 Wm^{-2} in CPTEC's atmospheric absorption is reduced to about 1 Wm^{-2} when CLIRAD is used, and UKMO seems to have an atmospheric aborption in excess of about 2 Wm^{-2}; for all-sky, however, CLIRAD fills only about half of CPTEC's gap, while UKMO fluxes are

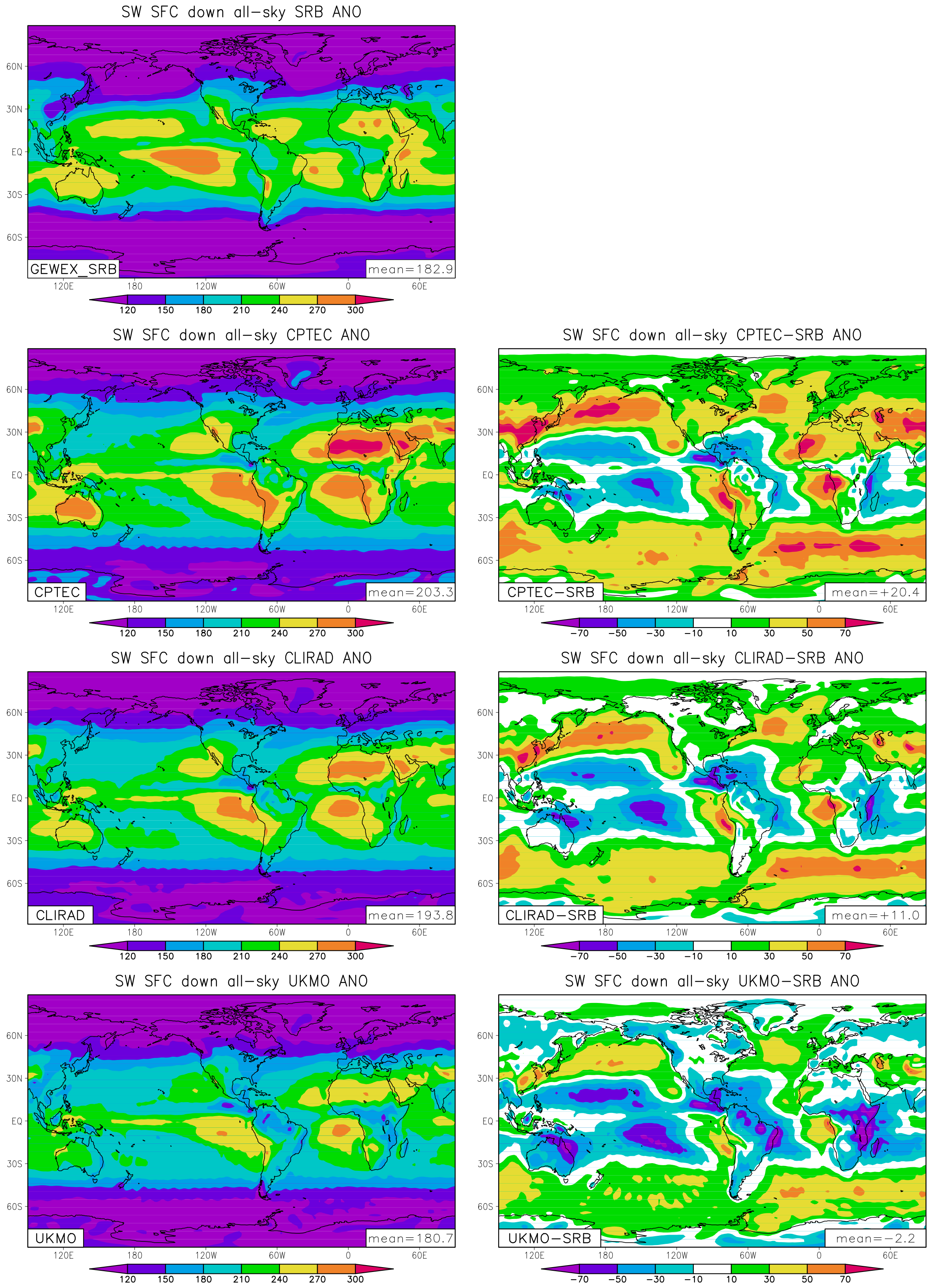

FIGURE 7.1 - Annual mean of the all-sky incident short wave at surface (Wm^{-2}). Top: generated by NASA/GEWEX SRB project; middle: calculated by current CPTEC AGCM and difference from SRB, calculated by CPTEC AGCM with CLIRAD-SW short-wave code and difference from SRB; bottom: calculated by CPTEC AGCM with UKMO radiation code and difference from SRB.

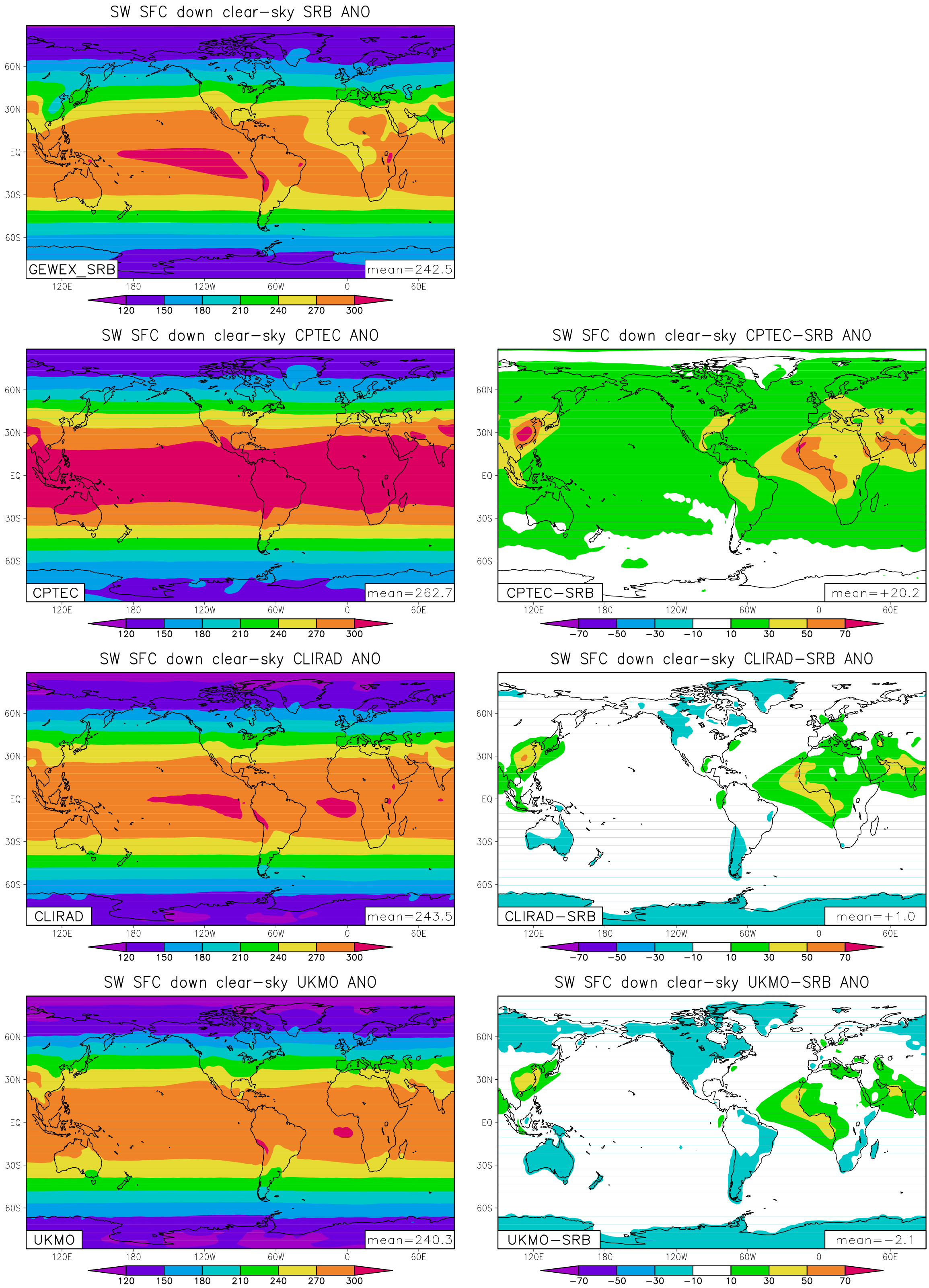

FIGURE 7.2 - Annual mean of the all-sky incident short wave at surface (Wm^{-2}). Top: generated by NASA/GEWEX SRB project; middle: calculated by current CPTEC AGCM and difference from SRB, calculated by CPTEC AGCM with CLIRAD-SW short-wave code and difference from SRB; bottom: calculated by CPTEC AGCM with UKMO radiation code and difference from SRB.

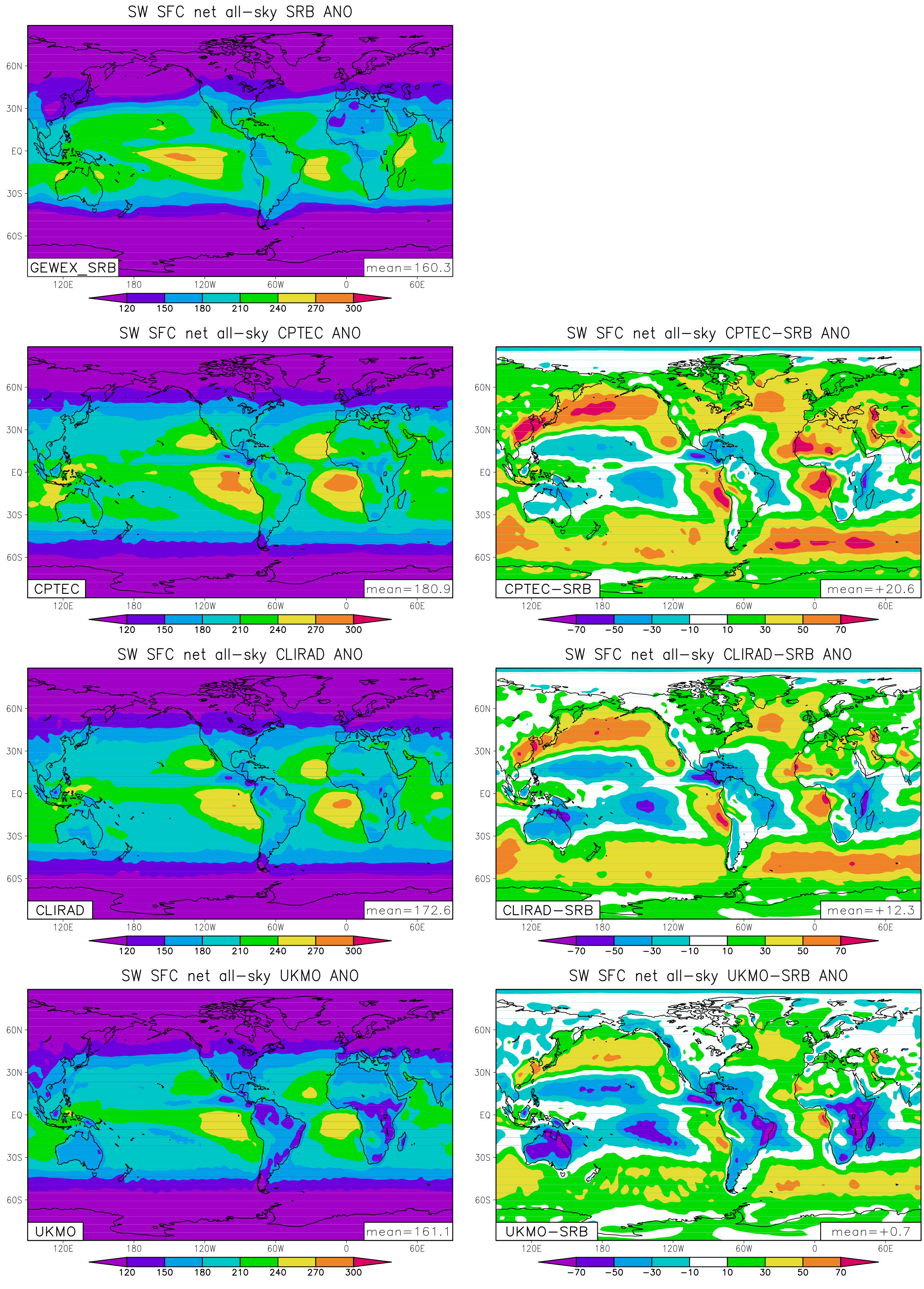

FIGURE 7.3 - Annual mean of the all-sky net short wave at the surface (Wm^{-2}). Top: generated by NASA/GEWEX SRB project; middle: calculated by current CPTEC AGCM and difference from SRB, calculated by CPTEC AGCM with CLIRAD-SW short-wave code and difference from SRB; bottom: calculated by CPTEC AGCM with UKMO radiation code and difference from SRB.

TABLE 7.1 - Global mean of short-wave fluxes (in Wm^{-2}) at top-of-atmosphere (TOA) and at surface (SFC) averaged over 1) a twelve-month (Dec/2002–Nov/2003) period, and two three-month periods, 2) Dec/2002–Feb/2003 and 3) Jun/2003–Aug/2003. SRB, CPTEC, CLIRAD and UKMO as described in the text.

	SRB	CPTEC–SRB	CLIRAD–SRB	UKMO–SRB
	1) 12-month: Dec/2002–Nov/2003			
TOA down all-sky	341.4	–0.0	–0.0	–0.0
SFC down all-sky	182.9	20.4	11.0	–2.2
SFC down clear-sky	242.5	20.2	1.0	–2.1
SFC net all-sky	160.3	20.8	12.3	0.7
	2) 3-month: Dec/2002–Feb/2003			
TOA down all-sky	350.2	1.6	1.6	1.6
SFC down all-sky	188.2	21.7	12.7	–0.7
SFC down clear-sky	252.9	18.8	–0.7	–3.7
SFC net all-sky	164.2	22.6	14.9	3.1
	3) 3-month: Jun/2003–Aug/2003			
TOA down all-sky	332.7	–1.6	–1.6	–1.6
SFC down all-sky	176.6	19.6	9.9	–4.0
SFC down clear-sky	230.7	22.5	3.7	0.2
SFC net all-sky	155.9	18.7	10.0	–2.4

very close to the satellite-derived figures. This behaviour is in accordance with the off-line results presented in Chapter 3.

7.2 Long-wave fluxes

The long-wave fluxes, as calculated by CPTEC, CLIRAD, and UKMO are compared with release 2.5 of the dataset produced by the NASA/GEWEX SRB Project. Figures 7.4 and 7.5 show respectively one-year-averaged global fields of 1) the upward long-wave all-sky flux at top-of-atmosphere and 2) the net long-wave all-sky flux at surface. Every figure shows seven plots of the appropriate field, one from the SRB dataset, taken as reference, and the other three pairs displaying the results of the three AGCM runs along with the differences of these runs and the SRB reference. Global means of the twelve-month and three-month averaged long-wave radiative fluxes are summarized in Table 7.2.

The main conclusions drawn from Table 7.2 are: long-wave fluxes are better represented by UKMO than by current CPTEC long-wave scheme. Differences, however, are small, specially if one considers that the overall error of SRB data is reported to be about 5 Wm^{-2}.

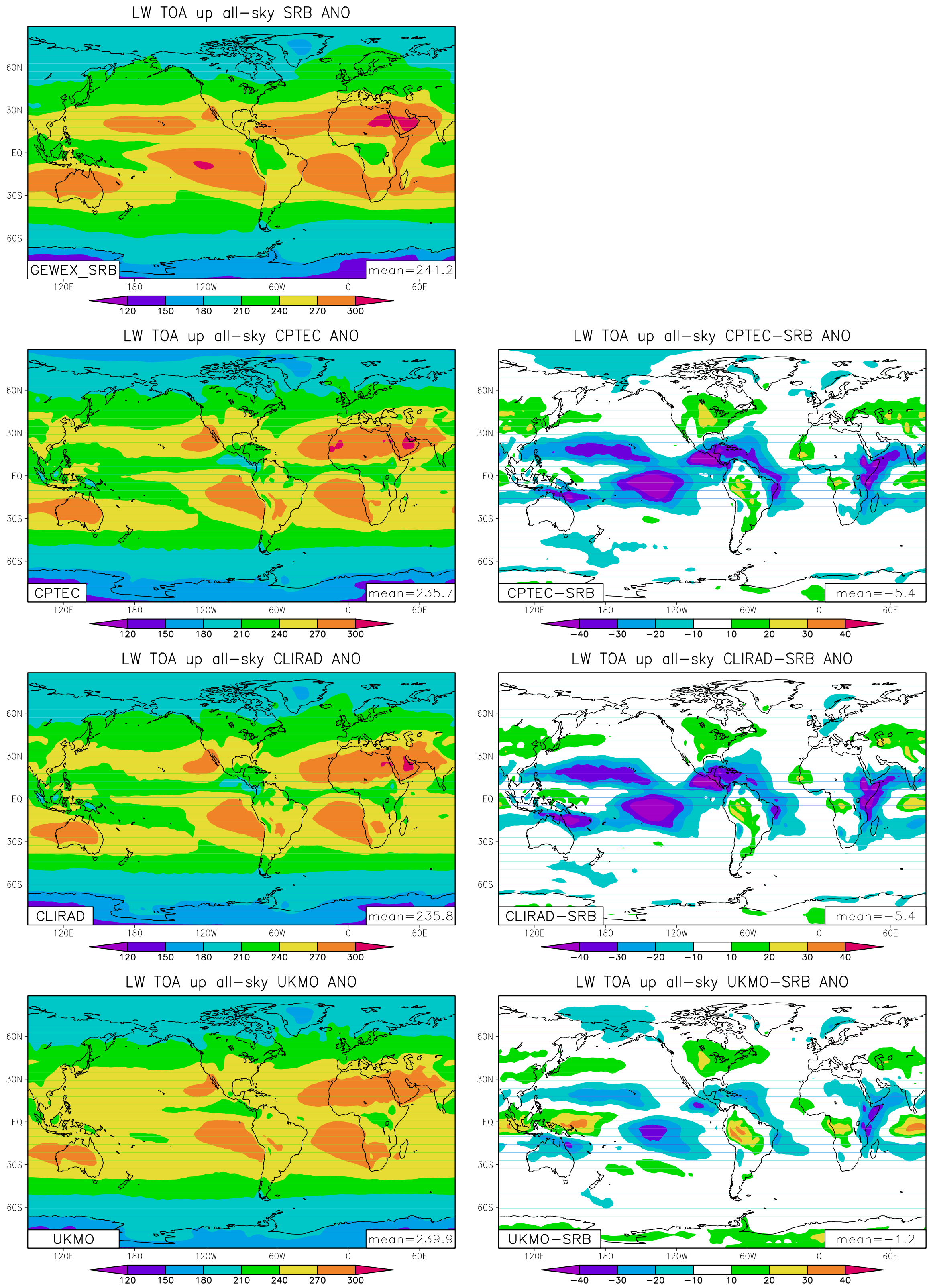

FIGURE 7.4 - Annual mean of the all-sky outgoing long wave at the top-of-atmosphere (Wm^{-2}). Top: generated by NASA/GEWEX SRB project, release 2.5; middle: calculated by current CPTEC AGCM and difference from SRB, calculated by CPTEC AGCM with CLIRAD-SW short-wave code and difference from SRB; bottom: calculated by CPTEC AGCM with UKMO radiation code and difference from SRB.

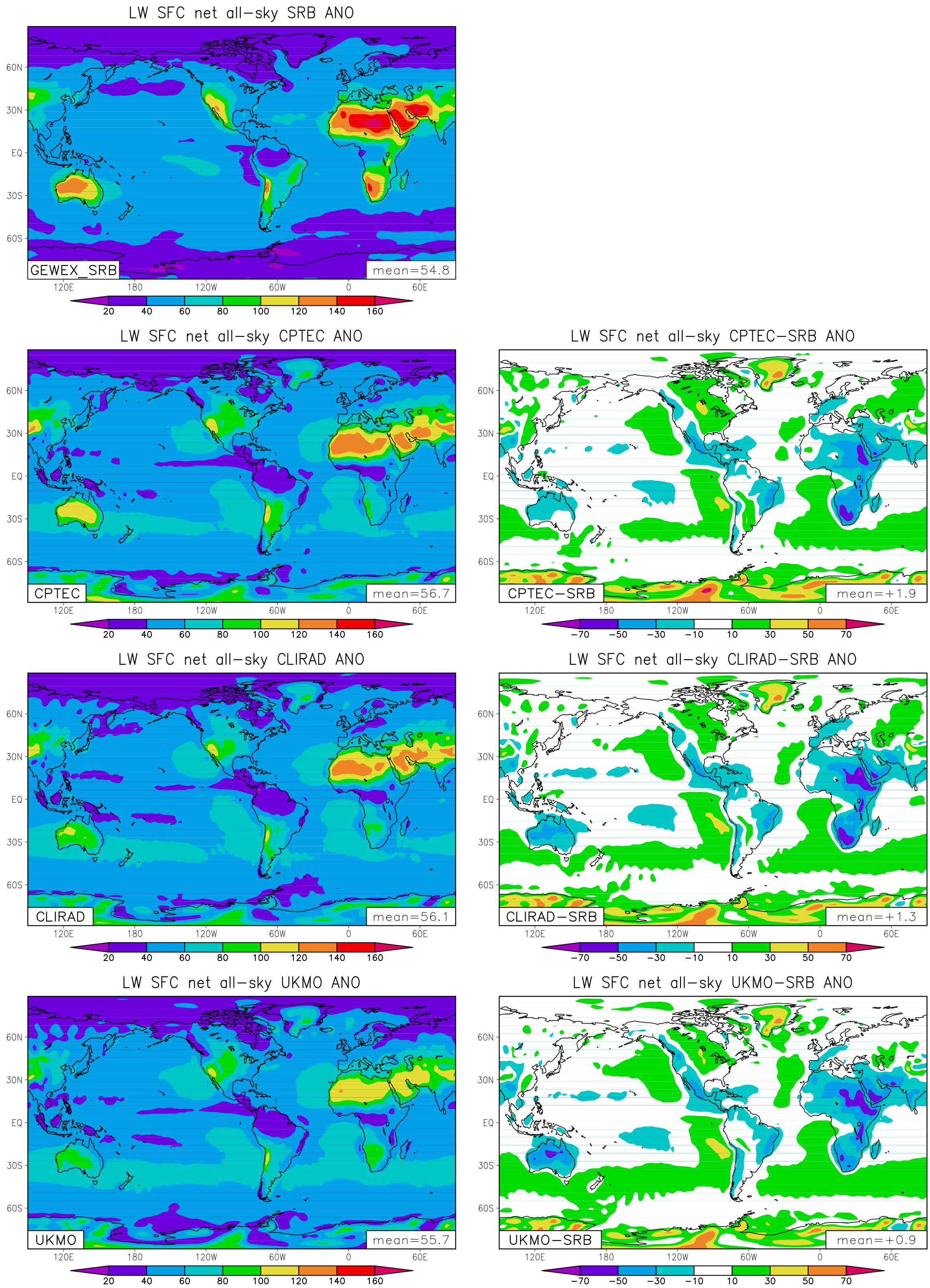

FIGURE 7.5 - Annual mean of the all-sky net long wave at the surface (Wm^{-2}). Top: generated by NASA/GEWEX SRB project, release 2.5; middle: calculated by current CPTEC AGCM and difference from SRB, calculated by CPTEC AGCM with CLIRAD-SW short-wave code and difference from SRB; bottom: calculated by CPTEC AGCM with UKMO radiation code and difference from SRB.

TABLE 7.2 - Global mean of long-wave fluxes (in Wm^{-2}) at top-of-atmosphere (TOA) and at surface (SFC) averaged over 1) a twelve-month (Dec/2002–Nov/2003) period, and two three-month periods, 2) Dec/2002–Feb/2003 and 3) Jun/2003–Aug/2003. SRB, CPTEC, CLIRAD and UKMO as described in the text.

	SRB	CPTEC–SRB	CLIRAD–SRB	UKMO–SRB
1) 12-month: Dec/2002–Nov/2003				
LW TOA up all-sky	241.2	–5.4	–5.4	–1.2
LW SFC net all-sky	54.8	1.9	1.3	0.9
2) 3-month: Dec/2002–Feb/2003				
LW TOA up all-sky	237.6	–4.1	–3.6	0.6
LW SFC net all-sky	52.1	3.6	3.6	2.6
3) 3-month: Jun/2003–Aug/2003				
LW TOA up all-sky	245.6	–6.6	–6.8	–2.8
LW SFC net all-sky	56.5	0.9	0.0	–0.7

7.3 Processing time

As mentioned before, a great advantage of the long-wave algorithm implemented in the UKMO radiation scheme is its low computational cost if compared to current operational CPTEC code. The amount of floating pointing operations needed for a single call of the UKMO long-wave radiation scheme is a linear function of the number of vertical levels while it is a quatric function for the original Harshvardhan algorithm currently operational at CPTEC. This is shown in the lower panel of figure 7.6 for two different horizontal resolutions. For more than 42 vertical levels, the UKMO scheme becomes faster than the original one ant that will represent a great save in computational time for the high resolutions used in operational weather forecasting. The top panel of figure 7.6 shows the computational cost but now as a function of the horizontal resolution. It is clear that for tipical weather forecasting resolutions, the UKMO is much faster, while for tipical climatic resolutions, it is just slightly slower than Harshvardhan.

This results, however, have been obtained with the original UKMO routines from Hadley Centre. These have now been optimized for the CPTEC supercomputer. For tipical climatic resolutions, a 20–25% reduction in the total computational time was obtained with the newly optimized code, as shown in figure 7.7.

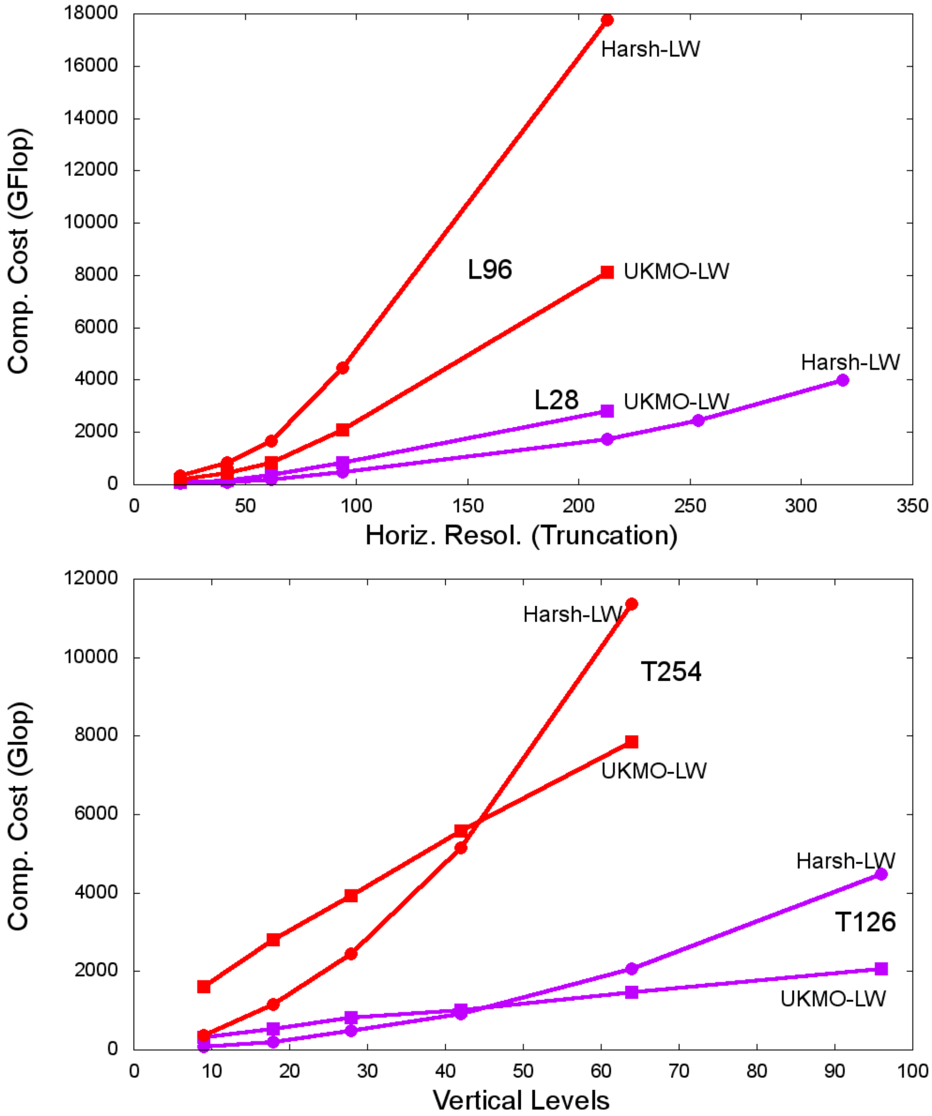

FIGURE 7.6 - Computational cost of CPTEC AGCM with Harshvardhan et al. (1987) and UKMO long-wave schemes, measured as the amount of floating pointing operations needed for a one day integration as a function of horizontal resolution (top) and number of vertical levels (bottom).

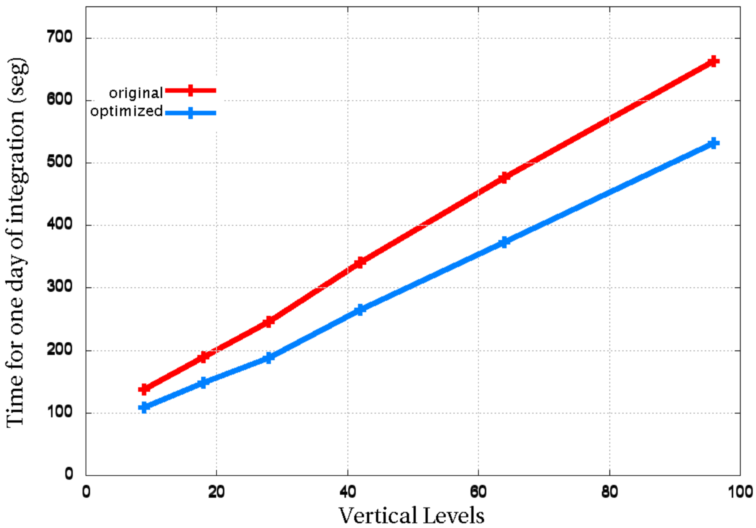

FIGURE 7.7 - Comparison between optimized and original UKMO radiation scheme. Plot shows the user time necessary for a one day integration of CPTEC GCM with T62 horizontal resolution and time-steps of 600s, as a function of vertical resolution.

8 CONCLUSION

Roughly speaking, the original radiation code of CPTEC's AGCM, based on Lacis e Hansen (1974) and Davies (1982) for short wave, and on Harshvardhan et al. (1987) for long wave, has two main drawbacks: low atmospheric short-wave absorption and high long-wave processing time. The low short-wave absorption results from the treatment of gaseous absorption, notably by the water vapor, from the crude evaluation of cloud extinction, and from the lack of aerosol effects. The use of the formulation of Ramaswamy e Freidenreich (1992) to estimate the water vapor short wave absorption, operational since 2004, only partially corrected the problem. The high processing time for long-wave calculations results from the method used where the number of calculations varies nearly quadratically with the number of atmosferic model layers.

The radiative transfer code of Edwards e Slingo (1996), operational at the UK Met Office and described in Chapter 2, was incorporated into CPTEC's AGCM in two steps. First, the short-wave code was assessed in off-line mode (Chapter 3) and it was found to be quite superior to the old and new operational CPTEC codes and to another code also incorporated into the AGCM, when compared with reference line-by-line calculations. The main reasons for this better performance is the improvement of gaseous absorption evaluation and specially the use of more sophisticated treatment of cloud extinction. Afterwards the short-wave code was incorporated into the AGCM (Chapter 5) and long-time comparative runs were performed (Chapter 6). This time, besides the new treatment of cloud extinction, a simplified aerosol climatology was added. When compared to satellite-derived short-wave radiation fields, results from the AGCM with UKMO code are much better than the results of current CPTEC code.

The second step was the incorporation of the long-wave code. Off-line tests were performed (Chapter 4) and it was found that the cooling rate profiles obtained with CPTEC and UKMO codes are quite similar and close to reference profiles obtained with line-by-line codes, and that UKMO produces long-wave fluxes closer to reference values than CPTEC. Then the long-wave code was incorporated into the AGCM and long-time runs were performed comparing current CPTEC for both short-wave and long-wave, CLIRAD for short-wave and CPTEC for long-wave, and UKMO for short-wave and long-wave (Chapter 7). As for the short-wave fluxes, the conclusions of these runs with the complete UKMO into the AGCM were quite similar to the conclusions of the first step. Incident short-wave at surface is badly modeled by CPTEC for both clear-sky and all-sky, with errors bigger than 20 Wm^{-2} associated with small atmospheric absorption. For clear-sky, the error is reduced to about 1 Wm^{-2}, when CLIRAD is used, and to –2 Wm^{-2} for the UKMO. For all-sky, CLIRAD's error is about 11 Wm^{-2}, and UKMO's keeps around –2 Wm^{-2}. As for the long-wave fluxes, they are better represented by UKMO than by current CPTEC long-wave scheme. Differences, however, are small. The main advantage of the new long-wave code is the reduction of the processing time.

REFERENCES

BARKER, H. W.; STEPHENS, G. L.; PARTAIN, P. T.; BERGMAN, J. W.; BONNEL, B.; CAMPANA, K.; CLOTHIAUX, E. E.; CLOUGH, S.; CUSACK, S.; DELAMERE, J.; EDWARDS, J.; EVANS, K. F.; FOUQUART, Y.; FREIDENREICH, S.; GALIN, V.; HOU, Y.; KATO, S.; LI, J.; MLAWER, E.; MORCRETTE, J.-J.; O'HIROK, W.; RäISäNEN, P.; RAMASWAMY, V.; RITTER, B.; ROZANOV, E.; SCHLESINGER, M.; SHIBATA, K.; SPORYSHEV, P.; SUN, Z.; WENDISH, M.; WOOD, N.; YANG, F. Assessing 1D atmospheric solar radiative transfer models: Interpretation and handling of unresolved clouds. **J.Climate**, v. 16, p. 2676–2699, 2003. 37, 41

BRIEGLEB, B. P. Delta-Eddington approximation for solar radiation in the NCAR Community Climate Model. **J. Geophys. Res**, v. 97, n. D7, p. 7603–7612, 1992. 19

CAVALCANTI, I. F. A.; MARENGO, J. A.; SATYAMURTY, P.; NOBRE, C. A.; TROSNIKOV, I.; BONATTI, J. P.; MANZI, A. O.; TARASOVA, T.; PEZZI, L. P.; D'ALMEIDA, C.; SAMPAIO, G.; CASTRO, C. C.; SANCHES, M. B.; CAMARGO, H. Global climatological features in a simulation using the CPTEC-COLA AGCM. **J. Climate**, v. 15, p. 2965–2988, 2002. 19, 37, 61

CHAGAS, J. C. S. **Comparações *off-line* de códigos radiativos de ondas curtas**. CPTEC/INPE, Cachoeira Paulista, 2006. 21 pp. 37

CHAGAS, J. C. S.; BARBOSA, H. M. J. Impact of UKMO's shortwave scheme on CPTEC's global model. In: AMERICAN METEOROLOGICAL SOCIETY. **The 12th Conference on Atmospheric Radiation**. Madison, Wisconsin, USA, 2006. Disponível em: <http://ams.confex.com/ams/pdfpapers/112861.pdf>. Acesso em: 22 out. 2008. 61

_____. Incorporation of UK Met Office's radiation scheme into CPTEC's global model. In: INTERNATIONAL RADIATION COMMISSION. **International Radiation Symposium 2008**. Foz do Iguaçu, PR, Brazil, 2008. Disponível em: <http://mtc-m18.sid.inpe.br/col/sid.inpe.br/mtc-m18%4080/2008/10.14.19.03/doc/109_manuscript.pdf>. Acesso em: 23 out. 2008. 69

CHAGAS, J. C. S.; MALAGUTTI, M.; NOBRE, P. Modificações no esquema de radiação do modelo global do CPTEC. In: SOCIEDADE BRASILEIRA DE METEOROLOGIA. **XIII Congresso Brasileiro de Meteorologia**. Fortaleza, Ceará, 2004. 19, 37

CHAGAS, J. C. S.; TARASOVA, T. A. **Parametrization of atmospheric radiation in the CPTEC/COLA general circulation model**. São José dos Campos: INPE, 1996. INPE-5980-NTC/327. 19, 53

CHOU, M.-D.; LEE, K.-T. Parameterizations for the absorption of solar radiation by water vapor and ozone. **J. Atmos. Sci.**, v. 53, n. 8, p. 1203–1208, 1996. 19

CHOU, M. D.; SUAREZ, M. J. **A solar radiation parameterization (CLIRAD-SW) for atmospheric studies**. NASA, TM-1999-104606, 40 pp, 1999. Series on Global Modeling and Data Assimilation, **15**. 20, 37, 38

CLOUGH, S. A.; IACONO, M. J.; MONCET, J.-L. Line-by-line calculations of atmospheric fluxes and cooling rates: Application to water vapor. **J.Geophys.Res.**, v. 97, p. 15761–15785, 1992. 37

CLOUGH, S. A.; KNEIZYS, F. X.; DAVIES, R. W. Line shape and the water vapor continuum. **Atmos. Res.**, v. 23, p. 229–241, 1989. 30, 38

CUSACK, S.; SLINGO, A.; EDWARDS, J. M.; WILD, M. The radiative impact of a simple aerosol climatology on the Hadley Centre atmospheric GCM. **Q. J. Roy. Meteorol. Soc.**, v. 124, p. 2517–2526, 1998. 20, 46, 57

DAVIES, R. **Documentation of the solar radiation parametrization in the GLAS climate model**. Greenbelt, MD, USA: Goddard Space Flight Center, 1982. NASA-TM-83961. 17, 19, 61, 62, 79

EDWARDS, J. M. Efficient calculation of infra-red fluxes and cooling rates using the two-stream equations. **J. Atmos. Sci.**, v. 53, p. 1921–1932, 1996. 31

EDWARDS, J. M.; SLINGO, A. Studies with a flexible new radiation code. I: Choosing a configuration for a large-scale model. **Q. J. Roy. Meteorol. Soc.**, v. 122, p. 689–719, 1996. 5, 7, 17, 20, 61, 62, 79

EDWARDS, J. M.; THELEN, J.-C. **Spectral files for the radiation scheme**. Exeter, UK: UK Met Office, 2003. Unified Model Documentation Paper No 23a. 23, 57

EDWARDS, J. M.; THELEN, J.-C.; INGRAM, W. J. **The radiation code**. Exeter, UK: UK Met Office, 2003. Unified Model Documentation Paper No 23. 23

ELLINGSON, R. G.; ELLIS, J.; FELS, S. The intercomparison of radiation codes used in climate models: Long wave results. **J. Geophys. Res.**, v. 96, n. D5, p. 8929–8953, May 1991. 11, 17, 47, 48, 50, 51

FOMIN, B. A.; GERSHANOV, Y. V. Preprint. **Tables of the benchmark calculations of atmospheric fluxes for the ICRCCM test cases. Part II: Long-wave clear-sky results**. Moscow: Kurchatov Institute, 1996. 11, 47, 48, 50, 51

FOUQUART, Y.; BONNEL, B.; RAMASWAMY, V. Intercomparing shortwave radiation codes for climate studies. **J. Geophys. Res.**, v. 96, n. D5, p. 8955–8968, 1991. 19, 37

GELEYN, J. F.; HOLLINGSWORTH, A. An economical analytical method for the computation of the interaction between scattering and line absorption of radiation. **Beiträge Phys. Atmosph.**, v. 52, p. 1–16, 1979. 32

HARSHVARDHAN; DAVIS, R.; RANDAL, D. A.; CORSETTI, T. G. A fast radiation parameterization for general circulation models. **J. Geophys. Res.**, v. 92, p. 1009–1016, 1987. 5, 7, 13, 19, 77, 79

HOU, Y.-T. **Cloud-radiation-dynamics interaction**. Tese — University of Maryland, 1990. 19

JOSEPH, J. H.; WISCOMBE, W. J.; WEINMAN, J. A. The delta-Eddington approximation for radiative flux transfer. **J. Atmos. Sci.**, v. 33, p. 2452–2459, 1976. 28

KIEHL, J. T. Sensitivity of a GCM climate simulation to differences in continental versus maritime cloud drop size. **J. Geophys. Res**, v. 99, p. 23107–23115, 1994. 11, 55, 56

KIEHL, J. T.; HACK, J. J.; BONAN, G. B.; BOVILLE, B. A.; BRIEGLEB, B. P.; WILLIAMSON, D. L.; RASCH, P. J. **Description of the NCAR Community Climate Model (CCM3)**. [S.l.], 1996. 54

KIEHL, J. T.; HACK, J. J.; BONAN, G. B.; BOVILLE, B. A.; WILLIAMSON, D. L.; RASCH, P. J. The national center for atmospheric research community climate model: CCM3. **J. Climate**, v. 11, p. 1131–1149, 1998. 42

LACIS, A. A.; HANSEN, J. E. A parameterization for the absorption of solar radiation in the Earth's atmosphere. **J. Atmos. Sci.**, v. 31, p. 118–133, 1974. 5, 7, 19, 79

LUTHER, F. M.; ELLINGSON, R. G.; FOUQUART, Y.; FELS, S.; SCOTT, N. A.; WISCOMBE, W. J. Intercomparison of radiation codes in climate models (ICRCCM): longwave clear-sky results — a workshop summary. **Bull. Am. Meteorol. Soc.**, v. 69, n. 1, p. 40–48, 1988. 37

McCLATCHEY, R. A.; FENN, R. W.; SELBY, J. E. A.; VOLZ, F. E.; GARING, J. S. **Optical properties of the atmosphere**. Bedford, Mass.: Air Force Cambridge Research Laboratory, 1972. Environ. Res. Paper 411. 19

MLAWER, E. J.; TOBIN, D.; CLOUGH, S. A. A new water vapor continuum model: MT_CKD_1.0. 2004. In preparation. 38

MONCET, J.-L.; CLOUGH, S. A. Accelerated monochromatic radiative transfer for scattering atmospheres: Application of a new model to spectral radiance observations. **J.Geophys.Res.**, v. 102, n. D18, p. 21853–21866, 1997. 37

NAKAJIMA, T.; HAYASAKA, T.; HIGURASHI, A.; HASHIDA, G.; MOHARRAM-NEJAD, N.; NAJAFI, Y.; VALAVI, H. Aaerosol optical properties in the Iranian region obtained by ground-based solar radiation measurements in the summer of 1991. **J. Appl. Meteorol.**, v. 35, p. 1265–1278, 1996. 58

PLANA-FATTORI, A.; SOUZA, E. P.; CHAGAS, J. C. S. Absorption of solar radiation by water vapor in the atmosphere. Part I: A comparison between selected parameterizations and reference results. **Rev. Bras. Geofísica**, v. 15, p. 275–290, 1997. 19

RAMASWAMY, V.; FREIDENREICH, S. M. A study of broadband parameterizations of the solar radiative interactions with water vapor and water drops. **J. Geophys. Res.**, v. 97, n. D11, p. 11487–11512, 1992. 5, 7, 17, 19, 61, 62, 79

RITTER, B.; GELEYN, J.-F. A comprehensive radiation scheme for numerical weather prediction models with potential applications in climate simulations. **Mon. Wea. Rev.**, v. 120, p. 303–325, 1992. 31

ROTHMAN, L. S.; BARBE, A.; BENNER, D. C.; BROWN, L. R.; CAMY-PEYRET, C.; CARLEER, M. R.; CHANCE, K.; CLERBAUX, C.; DANA, V.; DEVI, V. M.; FAYT, A.; FLAUD, J.-M.; GAMACHE, R. R.; GOLDMAN, A.; JACQUEMART, D.; JUCKS, K. W.; LAFFERTY, W. J.; MANDIN, J.-Y.; MASSIE, S. T.; NEMTCHINOV, V.; NEWNHAM, D. A.; PERRIN, A.; RINSLAND, C. P.; SCHROEDER, J.; SMITH, K. M.; SMITH, M. A. H.; TANG, K.; TOTH, R. A.; AUWERA, J. V.; VARANASI, P.; YOSHINO, K. The HITRAN molecular spectroscopic database: edition of 2000 including updates through 2001. **J.Quant.Spec.Rad.Trans.**, v. 82, p. 5–44, 2003. 37

ROTHMAN, L. S.; JACQUEMART, D.; BARBE, A.; BENNER, D. C.; BIRK, M.; BROWN, L. R.; CARLEER, M. R.; JR, C. C.; CHANCE, K.; COUDERT, L. H.; DANA, V.; DEVI, V. M.; FLAUD, J.-M.; GAMACHE, R. R.; GOLDMAN, A.; HARTMANN, J.-M.; JUCKS, K. W.; MAKI, A. G.; MANDIN, J.-Y.; MASSIE, S. T.;

ORPHAL, J.; PERRIN, A.; RINSLAND, C. P.; SMITH, M. A. H.; TENNYSON, J.; TOLCHENOV, R. N.; TOTH, R. A.; AUWERA, J. V.; VARANASI, P.; WAGNER, G. The HITRAN 2004 molecular spectroscopic database. **J.Quant.Spec.Rad.Trans.**, v. 96, p. 139–204, 2005. 38

ROTHMAN, L. S.; RINSLAND, C. P.; GOLDMAN, A.; MASSIE, S. T.; EDWARDS, D. P.; FLAUD, J.-M.; PERRIN, A.; CAMY-PEYRET, C.; DANA, V.; MANDIN, J.-Y.; SCHROEDER, J.; MCCANN, A.; GAMACHE, R. R.; WATSON, R. B.; YOSHINO, K.; CHANCE, K. V.; JUCKS, K. W.; BROWN, L. R.; NEMTCHINOV, V.; VARANASI, P. The HITRAN molecular spectroscopic database and HAWKS (HITRAN atmospheric workstation): 1996 edition. **J.Quant.Spec.Rad.Trans.**, v. 60, n. 5, p. 665–710, 1998. 38

SATO, N.; SELLERS, P. J.; RANDALL, D. A.; SCHNEIDER, E. K.; SHUKLA, J.; KINTER III, J. L.; HOU, Y.-T.; ALBERTAZZI, E. Effects of implementing the simple biosfere model in a general circulation model. **J. Atmos. Sci.**, v. 46, p. 2757–2782, 1989. 19

SLINGO, A.; SCHRECKER, H. M. On the radiative properties of stratiform water clouds. **Q. J. Roy. Meteorol. Soc.**, v. 108, p. 407–426, 1982. 31

SLINGO, J. M. The development and verification of a cloud prediction scheme for the ECMWF model. **Q. J. Roy. Meteorol. Soc.**, v. 113, p. 899–927, 1987. 55

SOUZA, E. P.; DIAS, P. L. S.; PLANA-FATTORI, A.; CHAGAS, J. C. S. Absorption of solar radiation by water vapor in the atmosphere. Part II: Sensitivity tests with a general circulation model. **Rev. Bras. Geofísica**, v. 15, p. 291–305, 1997. 19

TARASOVA, T.; FOMIN, B. Solar radiation absorption due to water vapor: Advanced broadband parameterizations. **J.Appl.Meteorol.**, v. 39, p. 1947–51, 2000. 20, 37, 38

TARASOVA, T. A.; CAVALCANTI, I. F. Monthly mean solar radiation fluxes and cloud forcing over South America in the period 1986–88: GCM results and satellite-derived data. **J. Appl. Meteorol.**, v. 41, p. 863–871, 2002. 19

TARASOVA, T. A.; FIGUEROA, S. N.; BARBOSA, H. M. J. **Incorporation of new solar radiation scheme into CPTEC GCM**. São José dos Campos, INPE, 2007. INPE-14052-NTE/371, 44 pp. 20, 37

WHITLOCK, C. H.; CHARLOCK, T. P.; STAYLOR, W. F.; PINKER, R. T.; LASZLO, I.; DIPASQUALE, R. C.; RITCHEY, N. A. **WCRP Surface radiation budget shortwave data product description - version 1.1**. [S.l.], 1993. 28 pp. 17, 61

WILD, M. Solar radiation budgets in atmospheric model intercomparisons from a surface perspective. **Geophys.Res.Lett.**, v. 32, 2005. L07704. 17, 61

WILD, M. et al. Evaluation of clear-sky solar fluxes in GCMs participating in AMIP and IPCC-AR4 from a surface perspective. **J.Geophys.Res.**, v. 111, 2006. D01104. 17, 61

WORLD METEOROLOGICAL ORGANIZATION. **Report of the meeting of JSC experts on aerosol and climate**. [S.l.], 1982. WCP-12. 57

_____. **Report of the experts meeting on aerosol and their climatic efects**. [S.l.], 1983. WCP-55. 57, 58

_____. **Atmospheric Ozone 1985, WMO global ozone research and monitoring project**. [S.l.], 1986. Report No. 16, Geneva. 38

ZDUNKOWSKI, W. G.; KORB, G. J. Numerische methoden zur lösung der stralungsübertragungsgleichung. **Promet**, v. 2/3, p. 26–39, 1985. 26

ZDUNKOWSKI, W. G.; PANHANS, W.-G.; WELCH, R. M.; KORB, G. J. A radiation scheme for circulation and climate models. **Beiträge Phys. Atmosph.**, v. 55, p. 215–238, 1982. 32

ZDUNKOWSKI, W. G.; WELCH, R. M.; KORB, G. An investigation of the structure of typical two-stream methods for the calculation of solar fluxes and heating rates in clouds. **Beiträge Phys. Atmosph.**, v. 53, n. 147–166, 1980. 27

PUBLICAÇÕES TÉCNICO-CIENTÍFICAS EDITADAS PELO INPE

Teses e Dissertações (TDI)

Teses e Dissertações apresentadas nos Cursos de Pós-Graduação do INPE.

Notas Técnico-Científicas (NTC)

Incluem resultados preliminares de pesquisa, descrição de equipamentos, descrição e ou documentação de programa de computador, descrição de sistemas e experimentos, apresentação de testes, dados, atlas, e documentação de projetos de engenharia.

Propostas e Relatórios de Projetos (PRP)

São propostas de projetos técnico-científicos e relatórios de acompanhamento de projetos, atividades e convênios.

Publicações Seriadas

São os seriados técnico-científicos: boletins, periódicos, anuários e anais de eventos (simpósios e congressos). Constam destas publicações o Internacional Standard Serial Number (ISSN), que é um código único e definitivo para identificação de títulos de seriados.

Pré-publicações (PRE)

Todos os artigos publicados em periódicos, anais e como capítulos de livros.

Manuais Técnicos (MAN)

São publicações de caráter técnico que incluem normas, procedimentos, instruções e orientações.

Relatórios de Pesquisa (RPQ)

Reportam resultados ou progressos de pesquisas tanto de natureza técnica quanto científica, cujo nível seja compatível com o de uma publicação em periódico nacional ou internacional.

Publicações Didáticas (PUD)

Incluem apostilas, notas de aula e manuais didáticos.

Programas de Computador (PDC)

São a seqüência de instruções ou códigos, expressos em uma linguagem de programação compilada ou interpretada, a ser executada por um computador para alcançar um determinado objetivo. São aceitos tanto programas fonte quanto executáveis.